General Disclaimer

One or more of the Following Statements may affect this Document

- This document has been reproduced from the best copy furnished by the organizational source. It is being released in the interest of making available as much information as possible.

- This document may contain data, which exceeds the sheet parameters. It was furnished in this condition by the organizational source and is the best copy available.

- This document may contain tone-on-tone or color graphs, charts and/or pictures, which have been reproduced in black and white.

- This document is paginated as submitted by the original source.

- Portions of this document are not fully legible due to the historical nature of some of the material. However, it is the best reproduction available from the original submission.

Produced by the NASA Center for Aerospace Information (CASI)

5 ϕr

NASA CR-156761

Present-Day Plate Motions

J. Bernard Minster

Seismological Laboratory
California Institute of Technology
Pasadena, California 91125

Thomas H. Jordan

Geological Research Division
Scripps Institution of Oceanography
La Jolla, California 92093

November 10, 1977

Submitted to Journal of Geophysical Research

(NASA-CR-156761) PRESENT-DAY PLATE MOTIONS (California Inst. of Tech.) 83 p HC A05/MF A01 CSCL 08F

N78-24709

Unclas
G3/46 21197

JUN 1978
RECEIVED
NASA STI FACILITY

JUN 1978
RECEIVED
NASA STI FACILITY
ACQ BRANCH

Abstract

A data set comprising 110 spreading rates, 78 transform fault azimuths and 142 earthquake slip vectors has been inverted to yield a new instantaneous plate motion model, designated RM2. The model represents a considerable improvement over our previous estimate RM1 (Minster, Jordan, Molnar and Haines, 1974). The mean averaging interval for the relative motion data has been reduced to less than 3 My. A detailed comparison of RM2 with angular velocity vectors which best fit the data along individual plate boundaries indicates that RM2 performs close to optimally in most regions, with several notable exceptions. The model systematically misfits data along the India-Antarctica and Pacific-India plate boundaries. We hypothesize that these discrepancies are manifestations of internal deformation within the Indian plate; the data are compatible with NW-SE compression across the Ninetyeast Ridge at a rate of about 1 cm/yr. RM2 also fails to satisfy the EW-trending transform fault azimuths observed in the FAMOUS area, which is shown to be a consequence of closure contraints about the Azores triple junction. Slow movement between North and South America is required by the data set, although the angular velocity vector describing this motion remains poorly constrained. The existence of a Bering plate, postulated in our previous study, is not necessary if we accept the proposal of Engdahl and others that the Aleutian slip vector data are biased by slab effects. Absolute motion models are derived from several kinematical hypotheses and compared with the data from hotspot traces younger than 10 My. Although some of the models are inconsistent with the Wilson-Morgan hypothesis, the overall resolving power of the hotspot data is poor, and the directions of absolute motion for the several slower-moving plates are not usefully constrained.

Introduction

Present-day plate motions can be modelled using systematic inversion methods. In our initial study (Minster *et al.*, 1974, referred to as Paper I), a linearized least-squares algorithm was formulated and applied to an extensive, globally distributed data set. Angular velocity vectors for eleven major plates were estimated from these data, and this model was designated Relative Motion 1 (RM1). The Caribbean plate was subsequently added to this model by Jordan (1975). Revisions and additions to the data set were begun in 1975, and an interim model was derived (Jordan, Minster and Molnar, 1976).

We present in this paper a new relative motion model, RM2, based on a much improved data set. Consistent with our previous work, we have attempted to obtain a *simple* model compatible with the available high-quality observations of relative motions. Only relative motion data which involve at least one oceanic plate have been used, since the data from intracontinental environments exhibit complexities not easily described in terms of rigid plate kinematics (e.g. Molnar and Tapponnier, 1975). We have not attempted to model the complex tectonics of the western Pacific (e.g., the Philippine plate), because little kinematical information is available concerning behind-the-arc spreading, and the assumptions fundamental to a simple plate model (e.g. triple-junction closure) may not apply.

The value of any model can be judged by its predictive capability and by its ability to withstand the test of new observations. In this respect the success of our original model RM1 has been mixed. For example, the relative motion between the North American and South American plates was predicted by RM1 entirely on the basis of data from other plate boundaries. Although no data yet exist which confirm directly the existence of such relative motion, the model implies that a component of NS convergence exists between the South American and Caribbean plates (Jordan, 1975). It appears that some convergence is indeed required by recent studies (Talwani et al., 1976; Rial, 1978).

On the other hand, RM1 failed to satisfy an extensive set of new data collected in the South Atlantic Ocean (Forsyth, 1975; Sclater et al., 1976). The investigation of this failure is an important aspect of this study. We show that RM1 incorrectly predicts the plate kinematics in the South Atlantic because the presently available data are inconsistent with the plate geometry assumed in deriving RM1. We demonstrate that this inconsistency can be remedied by postulating the existence of internal deformation with the Indian plate, although alternate explanations are possible.

Other problems with the RM1 model have been noted (Jordan et al., 1976). The well-mapped fracture zones in the FAMOUS area yield an apparent azimuth for Africa-North America motion that is due east (Macdonald and Luyendyk, 1977), whereas RM1 predicts an azimuth of S79E, parallel to the general trends of the nearby major transform faults (e.g. the Oceanographer T. F.).

In RM1 the slip vector data from the North Pacific were modelled using a Bering plate whose motion differs from that of North America. Engdahl et al. (1977) have demonstrated that the focal mechanisms from this region can be affected by slab structure, perhaps biasing the observations. They have suggested that corrections for this bias may eliminate the need for a Bering plate.

These and other problems are examined in this paper.

The Revised Data Set

The 330 data used in this study are listed in Table 1. The data locations are shown in Figure 1, delineating the major plate boundaries. These relative motion data comprise 110 rates of sea floor spreading derived from magnetic anomaly profiles, 78 transform fault azimuths and 142 earthquake slip vectors. In compiling and editing this data set, we have generally followed the guidelines in Paper I. In particular, we have excluded data from diffuse plate boundaries, specifically continent-continent boundaries. Therefore the details of Asian and Indonesian tectonics are not represented by our model.

Rate data have been determined directly from published magnetic anomaly profiles using the time scale of Talwani et al. (1971). In Paper I, anomalies 3 and 5 were generally used to estimate rates; we thus averaged the plate speeds over the last 5-10 My. In this study, we have redetermined the spreading rates using anomalies 2 and 2' in every instance, except for a few slow-spreading profiles where the anomalies out to 3 were employed. Hence, the mean averaging interval for the rate data is less than 3 My. In most cases the rates were determined by comparing the corrected profiles with synthetics, generally those published by the authors of the original observational study. However, for the anomaly profiles along the Pacific-Antarctic Ridge (Molnar et al., 1975), we generated our own synthetics. For the several studies where a direct inversion for magnetization was made (Macdonald, 1977; Macdonald and Holcombe, 1978; McGregor et al., 1977), the original authors' results were used directly.

In Paper I, the directions of plate motion implied by earthquake focal mechanisms were estimated by projecting the slip vectors onto a horizontal plane. Although this procedure is almost universally adopted, it is only approximately correct for shallow thrust events in subduction zones with oblique convergence, and it can introduce a slight bias. In this study, the more exact procedure of rotating the slip vectors into the horizontal plane was employed for earthquakes along inclined seismic zones. This problem is discussed in the Appendix.

The most precise estimates of relative motion direction are the azimuths of well-mapped transform faults. In determining these azimuths we have used detailed bathymetric surveys where available, relying on contours which cross charted ship tracks. Interpretive diagrams have been avoided to minimize the feedback between data and plate tectonic models.

The uncertainties listed in Table 1 are based on a case by case subjective evaluation of the data quality. They are used to weight the data in the inversion algorithm and to derive estimates of the uncertainties in the model parameters. Although we have attempted to use a consistent set of criteria in assigning these errors, the estimates are nevertheless crude indicators of data quality. With this in mind, we have adopted a conservative stand and have deliberately overestimated these uncertainties. This bias is apparent in Figure 3, where it is seen that the sample standard deviation of the normalized residual distribution is significantly less than its expected value of 1.

Model RM2: General Description

Inversion of the data was performed using the linearized, iterative, weighted least-squares algorithm described in Paper I. Our extensive experience in applying this algorithm to the plate motion problem has demonstrated to us its effectiveness. Although the algorithm involves the linearization of a non-linear problem, convergence has always been rapid and no difficulties associated with local minima have been evident. The uncertainties in the model parameters derived from the linear theory have proven to be effective measures of the errors induced on the model by errors in the data.

The inversion algorithm has been applied to the data set listed in Table 1 to obtain an 11 plate model, designated RM2. The plate geometry is identical to that of RM1, except that the Bering plate has been recombined with the North American plate and a Caribbean plate has been added. RM1, supplemented with the CARB-NOAM angular velocity vector derived by Jordan (1975), was used as a starting model in the inversion algorithm. Convergence was attained in five iterations.

Model RM2 is specified in Table 2 by its geohedron (McKenzie and Parker, 1974). Although a more compact specification is possible, this format conveniently provides an explicit relative rotation vector for each plate boundary. The RM2 geohedron is illustrated in Figure 2.

In the notation of Paper I the quantity minimized by the fitting procedure is the variable

$$\chi^2 = \sum_{i=1}^{N} \frac{[d_i^o - d_i(\underset{\sim}{m})]^2}{\sigma_i^{\,2}}$$

where N = 330 is the total number of data. The eleven plate model is specified by 30 parameters. If the data were normally distributed and the variances were exactly known, χ^2 would be chi-square distributed with 300 degrees of freedom, and a sample value would lie in the interval (300 ± 49) 95% of the time. The value of χ^2 for RM2 is 109, almost a factor of three less than its expected value. Thus, the data are fitted significantly better than they should be if their assigned uncertainties were correct.

This fact is also evident from the histograms of normalized residuals plotted in Figure 3. The sample variances of these distributions are about 1/3 their expected value of unity. This discrepancy could be corrected by uniformly reducing the standard errors assigned to the data by a factor of $1/\sqrt{3}$. Such a reduction would not change the model but would decrease the derived model uncertainties by the same factor. However, to be conservative we have retained the larger estimates of uncertainty.

It can be seen from Figure 3 that the distribution of normalized residuals for the slip vector data departs from the assumed gaussian behavior in another manner: the distribution is skewed towards negative values. Much of this skewness is attributable to the predominantly negative residuals exhibited by the slip vectors from the Aleutians and the Kurils, a feature discussed in more detail below.

Because the data set is large and because the geometry of the problem is complex, the performance of RM2 cannot be fully described by these simple statistics. A complete assessment of RM2's success in explaining the observations requires that each data subset pertaining to an individual plate boundary be considered separately. For a large number of plate pairs, a relative rotation vector, or at least a "best-fitting pole" (BFP), can be determined from that data subset alone. These vectors and poles have been obtained by inversion and are listed in Table 3. The corresponding BFP's are shown with the RM1 and RM2 poles on Figures 4-6. The differences between these poles and those for RM2 measure the constraints imposed on RM2 by the simultaneous inversion scheme. These differences are not large, which is evidence that RM2 performs close to optimally in most regions. Notable exceptions involve the INDI-ANTA, INDI-PCFC and AFRC-NOAM poles, discussed below.

The estimated model uncertainties σ_θ, σ_ϕ, σ_ω are much smaller in Table 2 than in Table 3. This is, of course, a direct consequence of the self-consistency constraints inherent to the rigid plate model, as discussed in Paper I. An impressive example of this behavior is provided by the COCO-PCFC rotation vector, which is heavily constrained by two triple junction closure conditions; these constraints reduce the nominal uncertainty of the rotation rate by a factor of four.

It should be emphasized that the uncertainties in the model parameters given in Table 2 correspond to marginal distributions. A complete description of the model uncertainties, including the various error cross-correlations, requires the specification of a 30 × 30 (symmetric) variance matrix. A more complete discussion of this point is given in Paper I.

Listed in Table 1 are quantities which we have termed "data importances." As defined in Paper I, they are the diagonal elements of an orthogonal projection operator in the data space, and are indicative of the distribution of information among the data (Paper I; Minster et al., 1977). Importances are additive and sum to the number of inverted parameters, 30 in the case of RM2. They depend on the geometry of the data set, and on the data uncertainties, but not on the actual values of the data. The final model depends heavily on the most important data and is robust with respect to the least important data.

Cumulative importances for individual plate boundaries are listed by data types in Table 2 for RM2 and in Table 3 for the best fitting vectors. The cumulative importance for all slip vector data is only 4.6, compared with 11.1 for the transform fault azimuths, despite the fact that the former outnumber the latter by nearly 2:1. This reflects the lower uncertainties--by a factor of two to three--generally assigned to transform fault data. The most important datum (0.95) is the rate across the Mid-Cayman Rise (Macdonald and Holcombe, 1978); alone, it essentially determines the relative speed of NOAM-CARB. When the entire data set is considered, 50% of the cumulative importance is associated with the 49 most important data, and only 10% with the 151 least important data. Importances are very useful for a detailed comparison of data and models, as illustrated in the next sections.

Model RM2: Detailed Assessment

This discussion is devoted to a detailed evaluation of RM2 on a region-by-region basis. The fit of RM1 and RM2 to the data for individual plate boundaries is illustrated in Figures 7-20. The data and model values are depicted as residuals with respect to the best-fitting angular velocity vectors and poles listed in Table 3. Baselines provided by the best-fitting vectors remove the large variations in the data functionals due to geometrical complexities and allow the models to be plotted as smooth lines on the diagrams. More importantly, the deviations from the locally best-fitting parameters required by closure conditions are readily apparent.

The Pacific-North America Boundary. It was concluded in Paper I that the slip-vector data along the Aleutian-Kuril trench system are not consistent with the NOAM-PCFC relative motion inferred from data in the Gulf of California and in the northwest Pacific. We suggested that this inconsistency was diagnostic of deformation of the North American plate, and attempted to model it by including a hypothetical Bering plate in RM1. However, the BERI-PCFC pole was determined by only ten slip vectors. Engdahl et al. (1977) pointed out that our data were a poor representation of the earthquake population along the trench and that the slip vector orientations for individual events in the vicinity of 175°E could be significantly biased by the laterally heterogeneous seismic velocity structure of the downgoing slab. In the present study the number of data along this trench system has been increased to 27, including 15 high quality slip vectors from the Kuril-Kamchatka Arc

ORIGINAL PAGE IS
OF POOR QUALITY

recently published by Stauder and Mualchin (1976). Because of the evidence for bias due to slab structure presented by Engdahl et al. (1977), we assigned large uncertainties (±20°) to the data lying between 165°E and 165°W longitude. It can be seen from Figure 7 that these data are in fact systematically misfit by RM2 and the BFP in the direction observed in Paper I and predicted by the model of Engdahl et al. (1977). On the other hand data from the Kuril-Kamchatka Arc are fitted by the model without difficulty, consistent with the conclusion of Engdahl et al. (1977) that slip vectors in this region are not likely to be significantly biased by slab structure. Since the fit of the data elsewhere along the boundary is satisfactory (Figure 7), we conclude that there is little evidence for deformation within the North American plate of the sort hypothesized in Paper I.

The East Pacific Rise. The data set for the COCO-PCFC boundary includes a redetermination of the Siqueiros T.F. azimuth from revised bathymetry (Rosendahl, 1976). RM2 performs very well along this boundary and constitutes a slight improvement over RM1 (Figure 8).

The data set for the NAZC-PCFC boundary has been significantly revised and augmented, especially the rate data set. Between 6°S and 12°S, the magnetics are poor and the data relatively scattered (Figure 9), as might be expected for east-west profiles in the vicinity of the magnetic equator. Nevertheless, Rea's (1976a, b) data indicate a lower rate than used in Paper I. Herron's (1972) profile at 19°S is easily readable, despite the small size of the published figure, but the bathymetry indicates that a fracture zone may be crossed to the west of the ridge. Thus, the western part of the profile is suspect beyond anomaly 2, and we assigned a large uncertainty to the measurement. A sequence of high quality profiles at 20°S has been discussed by Rea and Blakely (1975). Since their published profiles are rate adjusted and could not be remeasured, we adopted their estimated spreading rate (16.1 cm/yr) and assigned it an uncertainty of 0.6 cm/yr, a conservative value in view of the datum's quality. However, this rate is less than that obtained at 19°S and is not fitted well by the model. It is also difficult to reconcile this rate with the comparable rates much further north and a higher rate to the south: the profile at 28°S (Herron, 1972) yields a rate which exceeds 17 cm/yr.

The azimuths along the NAZC-PCFC boundary have been much improved by the recent bathymetric studies of Mammerickx *et al.* (1975) and Lonsdale (1977, 1978). However, the position of the NAZC-PCFC pole has not been significantly altered by these revisions; the RM1 and RM2 poles, and the BFP, lie very close together, well within the RM2 error ellipse.

The Galapagos Spreading Center. The rate data along the COCO-NAZC boundary are taken from the study by Hey (1974). We also included a good deep-tow profile published by Klitgord and Mudie (1974). As seen in Figure 10 and in Table 1, the data along this boundary are internally consistent. A particularly satisfying feature is that the recent bathymetry of Lonsdale and Klitgord (1978) clearly requires the COCO-NAZC pole to lie north of the equator; the transforms at 84.5°W and 85.3°W trend east of north. The implied shift from the RM1 pole position is in complete concordance with the shift dictated by the lower spreading rates along the NAZC-PCFC boundary. It should be noted that the strike of the Panama T.F. is very consistent with this new pole position, a point we shall return to in the next section.

The Chile Rise. The slower opening rate along the NAZC-PCFC boundary also affects the motion along the Chile Rise. In particular, the RM2 rate is considerably less than the 7.6 cm/yr estimate derived from the profile of Klitgord *et al.* (1973), which we consider to be the best rate observation along this boundary and is the only value included in the data set. However, the RM2 rate is between this value and the lower estimates of Morgan *et al.* (1968) and Herron and Hayes (1969).

Eastern Pacific Subduction Zones. Strongly coupled to the opening of the East Pacific Rise are the convergence rates and directions along the Middle American and South American trenches. We have adopted a set of slip vectors estimated by Stauder (1973, 1975) and Abe (1972) to represent the direction of subduction in South America. The residuals for these data show a slightly negative trend, although Abe's (1972) well determined solution has a large positive residual. The negative trend could be eliminated by increasing the rate along the NAZC-PCFC boundary. However, the COCO-NOAM and COCO-CARB slip vectors also exhibit this negative residual trend, and the possibility that these data are biased, like the Aleutian slip vectors, cannot be discounted. In any case, the scatter in the data is large, the average misfit is small and the data importances are low; hence, any bias will not significantly affect the model.

The Pacific-Antarctic Ridge. Because it is a keystone of the global model, particular attention was devoted to the PCFC-ANTA boundary. The data along this boundary are of sufficient number and quality to provide significant coupling, via the Antarctic plate, among the plates in the Pacific and the plates with boundaries in the South Atlantic and Indian Oceans. The configuration of the PCFC-ANTA boundary has been investigated by Molnar et al. (1975), and our data set is based primarily on this study. Since these authors did not use synthetic magnetic profiles, we computed synthetics and reinterpreted the magnetics. A significant component of apparently asymmetric spreading is observed on many profiles (Molnar et al., 1975; Stein et al., 1977), so the rates were estimated only from pairs of corresponding anomalies on both sides of the axis. All measurements were based on anomaly 2' or younger anomalies. Transform fault azimuths were derived from the bathymetry of Molnar et al. (1975), but estimates were obtained from ship track crossings rather than their interpretive map. It is clear from Figure 11 that RM2 is very close to the best-fitting vector and represents an improvement over RM1 in this region. The difference in the RM1 and RM2 poles is mainly attributable to the southwesternmost transform fault, an important datum ($\mathcal{J} = 0.25$) not included in Paper I. Some internal inconsistency of unknown origin is evident in the rate data (Figure 11): the rates are greater in the middle of the boundary than those required by the rates at the ends of the boundary. Nevertheless, most of the data are fitted within their uncertainties, and the relative rotation vector is one of the best determined in the RM2 geohedron.

The India-Pacific boundary. The data used along this boundary, consisting entirely of earthquake slip vectors, are the same as in Paper I, but the data north of 25°S were eliminated because of documented behind-the-arc spreading in the Lau Basin (e.g. Lawver et al., 1976). Nevertheless, the geometry is such that a BFP could be determined from the 14 remaining slip vectors (Table 3). We observe that this best-fitting pole is almost identical to the pole determined by Falconer (1973) exclusively from seismicity data along the Macquarie Ridge, a completely independent data set. However, as seen in Figures 4 and 12, both RM1 and RM2 differ significantly from this pole, a direct result of requiring closure around the INDI-PCFC-ANTA triple junction. Consequently, the global models are a poor fit to the southernmost slip vectors, determined by Banghar and Sykes (1969). Furthermore, these models predict a significant component of compression across the Macquarie Ridge system, in disagreement with the hypothesis of Falconer (1973) that this segment is a strike-slip fault. We strongly suspect that these inconsistencies result from internal deformation within the Indian plate (see below).

Motions about the Azores triple junction. The plate boundaries which form the Azores triple junction are individually well constrained. Figure 13 is a residual plot for the northern Mid-Atlantic Ridge data. The longitude of the EURA-NOAM pole is reasonably well fixed by the precise azimuth data along the Charlie-Gibbs T.F. and a number of fault plane solutions in the Arctic, but its latitude is more uncertain. Both the RM1 pole and the BFP lie near the mouth of the Lena River, the position most compatible with the rate data. The RM2 pole is several degrees further south (65.8°N, 132.4°E), and its fit to the rate data south of 60°N is not as good. However, this pole is more consistent with the conclusions reached by Chapman and Solomon (1976) in their study of northeast Asian tectonics.

The data set along the Azores-Gibraltar Line is considerably improved over our previous study. We deleted the datum east of Gibraltar, because of its probable involvement with the Alboran plate (Andrieux et al., 1971), but added three new slip vectors west of Gibraltar. The most important addition, however, is the azimuth of the Gloria T.F. ($\mathcal{I}$ = 0.783), well defined by Laughton et al. (1972) and Laughton et al. (1975). This datum places a strong constraint on the longitude of the AFRC-EURA pole. Although the individual slip vectors are not particularly well determined, their variation from NW compression on the east to SW extension on the west requires that the pole be not far south of the boundary, a conclusion established by McKenzie (1972). As a result, the pole is very tightly constrained, and the RM2 solution is very close to the BFP (Figures 6 and 14).

The data set south of the Azores on the Mid-Atlantic Ridge has also been improved. Several special studies have yielded much better magnetics, and these imply a significantly lower rate during the last 3 My than used in Paper I. The azimuth data along the AFRC-NOAM boundary have also been revised. In Paper I, the general trends of the Oceanographer T.F. (S77E) and the Atlantis T.F. (S81E) were used and were well fitted by RM1. In the present data set, these azimuths have been deleted and replaced by the azimuths of transforms A(S88E) and B(S89E) in the FAMOUS area (Macdonald and Luyendyk, 1977). The difference between the azimuths of the major transform faults and transforms A and B has been attributed to a change in the direction of plate motion within the last 5 My (Macdonald, 1977; Fox et al., 1978; Atwater and Macdonald, 1977). A slip vector showing east-west motion on the Oceanographer T.F. (Udías et al., 1976), supporting this conclusion, has also been included.

The revised data along the AFRC-NOAM boundary are internally consistent, as indicated by the performance of the best-fitting angular velocity vector, but the AFRC-NOAM azimuth data are poorly fitted by RM2 (Figure 15). It is clear that the misfit is forced by the closure condition about the Azores triple junction. To satisfy the triple junction condition, the AFRC-NOAM pole must be on the great circle connecting the EURA-NOAM and AFRC-EURA poles (Figure 4 & 6). The BFP is not; it lies to the west near the northeastern tip of Greenland, as required by the revised azimuth data. The triple junction great circle cannot be shifted to include the AFRC-NOAM BFP without completely misfitting the data along one or both of the other boundaries. For example, any good fit to both the AFRC-NOAM and EURA-NOAM data sets yields an AFRC-EURA pole that is much to the west of the RM2 pole and implies compressive motion along the entire Azores-Gibraltar Line, a prediction in flagrant disagreement with the observed earthquake mechanisms. Hence, the RM2 solution is significantly different from the AFRC-NOAM BFP. The RM1 and RM2 poles are each included within the other's 95% confidence ellipses. Both models predict directions of AFRC-NOAM motion which match the observed general trend of the Oceanographer T.F but which misfit the azimuths of transforms A and B by about 10°.

A possible explanation for this discrepancy concerns the way the RM2 data set averages over time. It is conceivable that the east-west trends observed in the FAMOUS region are so recent that the pole shifts required by this reorientation are not represented in the data from the other plate boundaries.

However, we believe that this explanation can be rejected. The location of the great circle connecting the EURA-NOAM and AFRC-EURA poles is fixed by truly "instantaneous" data; i.e., the slip vectors in the North Atlantic and along the Azores-Gibraltar Line. Therefore, the conflict is among data which involve little or no time averaging.

Perhaps the east-west transforms observed in the FAMOUS area are not unbiased indicators of AFRC-NOAM motion. This would be the case, for example, if these short fault segments were "leaky" in the sense of Menard and Atwater (1969); i.e., if a component of extension existed across these faults. For this explanation to be correct, the rate of opening normal to the faults would have to be about 0.4 cm/yr. Although the field data do not appear to support this hypothesis (Detrick et al., 1973; ARCYANA, 1975; Choukroune et al., 1977), the ability of these studies (as well as ours) to resolve such a component is an open question.

The incompatibility of the FAMOUS trends with the RM2 model remains problematic. It is interesting to note, however, that the RM2-predicted azimuths are essentially perpendicular to the rise-crest segments in the FAMOUS area.

The Americas: one plate or two? A major conclusion of Paper I was that significant relative motion exists between North and South America. The present study supports this conclusion, although direct observational evidence for NOAM-SOAM motion is still lacking. An inversion of the global data set was performed with the Americas grouped into a single plate. This model was rejected because it does not satisfy the relative motion data in the Atlantic. In particular:

(1) The rate data along the AFRC-NOAM boundary are misfit, model values being 0.4 cm/yr too low.

(2) The azimuths along the AFRC-SOAM boundary yield systematically positive residuals of about 5°.

(3) The EURA-NOAM pole is shifted northward to 81°N, 118°E, well outside the RM2 95% confidence ellipse. Consequently, the variation in rates along this boundary does not match the observations.

(4) The AFRC-EURA pole is shifted westward to 12°S, 38°W. Such a pole implies compressive motion along the entire Azores-Gibraltar Line. As noted above, this consequence is in direct conflict with the extension observed on the western portion of this boundary.

We conclude that a non-zero NOAM-SOAM angular velocity is required by the revised data set. To derive RM2, we adopted the convention of Paper I and partitioned the AFRC-NOAM and AFRC-SOAM data sets at 15°N, where the distance between the Mid-Atlantic Ridge and the West Indies Arc is least.

This grouping affords an excellent fit to the data along the AFRC-SOAM boundary (Figure 16). One datum on this boundary deserves particular mention: Eittreim and Ewing (1975) have mapped a recent, apparently continuous fault within the Vema fault zone. Their data yield a remarkably well determined azimuth of relative motion; we assigned this datum an uncertainty of $\pm 2^{o}$, the lowest given to any direction datum. Its residual computed from RM2 is only 0.4^{o}. In contrast, the residual computed from the model with a single Americas plate is nearly 5^{o}.

Although some motion is required, the NOAM-SOAM angular velocity vector is not precisely constrained. This is indicated by the large confidence ellipse associated with the pole (Figure 5). It is also evidenced by the fact that the RM2 pole is nearly 30^{o} north of the RM1 pole, completely reversing the sense of motion predicted along the boundary postulated to lie somewhere between 10^{o}N and 20^{o}N. Discussion of the inferred relative motion may be found in a later section.

Caribbean plate motion. Although a Caribbean plate was not included in the RM1 model derived in Paper I, the topic of Caribbean plate motion was treated in detail by Jordan (1975). He derived a NOAM-CARB angular velocity vector using a spreading rate of 2.2 cm/yr across the Mid-Cayman Rise estimated from topographic decay (Holcombe *et al.*, 1973). For the present study, we were fortunate to have available a much more reliable rate (2.0 ± 0.4 cm/yr since 2.3 My B.P.) determined from a magnetic profile across the Mid-Cayman Rise by Macdonald and Holcombe (1978).

This rate is essentially identical to the previous estimate. Four slip vectors from the Molnar and Sykes (1969) set used by Jordan (1975) were deleted, one from the West Indies Arc, because it may lie south of the CARB-NOAM-SOAM triple junction, and three from Hispaniola and the Puerto Rico Trench, where the data show internal scatter and the stress and strain fields are complex (Jordan, 1975). A slip vector for the 1976 Guatemala earthquake (Kanamori and Stewart, 1977) was added. The changes to the direction data shifted the NOAM-CARB pole northwestward from the position computed by Jordan (1975). It can be seen from Figure 5, however, that this shift is in the direction least constrained by the data, as indicated by the orientation of the RM2 confidence ellipse. Jordan's pole lies within this confidence ellipse, and the difference between these poles is not resolvable by the present data set (Figure 17).

The CARB-SOAM pole is also shifted with respect to Jordan's solution, but, again, the shift is along the major axis of the error ellipse. This pole is unconstrained by data along the CARB-SOAM boundary, so its 95% confidence ellipse is quite large. The change in its location reflects the shifts in both the NOAM-SOAM and NOAM-CARB poles. Nevertheless, Jordan's conclusion that a component of north-south motion exists along this boundary is unaffected (Table 5).

<u>The Bouvet triple junction.</u> RM1 did not predict correctly the relative motions of SOAM-ANTA and AFRC-ANTA (Forsyth, 1975; Sclater *et al.*, 1976). In Paper I, these boundaries were very poorly constrained by data, but this deficiency has been remedied by a number of recent

special studies (Table 1). RM2 provides an excellent fit to the data around Bouvet triple junction (Table 1, Figures 16 and 18), whereas RM1 performs miserably. Three explanations for this discrepancy were investigated:

(1) RM1 is located in a local minimum of the fitting function manifold. This possibility can be dismissed; inverting the RM1 data set with RM2 as a starting model yields the published RM1 solution.

(2) The SOAM-ANTA and AFRC-ANTA vectors are very sensitive to small errors in the RM1 data set. This possibility can also be excluded; the error ellipsoids for these vectors are actually quite small (Paper I, Table 2, Figures 5 and 7). The prediction error computed from the RM1 variance matrix is much smaller than the RM1 misfit to the new data. If the new data along the SOAM-ANTA and AFRC-ANTA boundaries are exluded from the revised data set, a solution similar to RM1 is obtained.

(3) The global data set is inconsistent with the plate geometry assumed by RM1.

Hypothesis (3) is our preferred explanation and was in fact advocated by Forsyth (1975) in his original study of this problem. For reasons detailed below, we believe that the data sets for plate motions about the Indian triple junction are inconsistent with our model, and we ascribe this inconsistency to internal deformation within the Indian plate.

Plate motions in the Indian Ocean. This brings us to the major difficulty we encountered in constructing RM2: as pointed out by Jordan et al. (1976) and Minster and Jordan (1977), each of the three legs of the Indian triple junction are populated by internally consistent data, but the three best-fitting vectors sum to a vector (the closure vector) significantly different from zero (Table 3, Figure 6).

The AFRC-ANTA boundary is densely populated by good observations. The 6 rates, 6 transform faults, and 11 slip vectors along this boundary constrain the angular velocity vector very well. The most important of these data is the well mapped Melville transform fault ($\delta = 0.53$) near the northeastern end of the boundary (Engel and Fisher, 1975), which controls the latitude of the pole. RM2 performs close to optimally along this boundary (Figure 18).

As noted by McKenzie and Sclater (1971), the transform faults along the Central Indian and Carlsberg ridges tightly constrain the INDI-AFRC pole, and these constraints have been strengthened by improved bathymetry (Engel and Fisher, 1975). As shown on Figure 19, there is a minor discrepancy between the rate data and the transform fault azimuths: the northernmost rates are too large by a few tenths of a cm/yr. In an effort to fit these rates, the best-fitting vector skews slightly with respect to the T.F. data, and RM2 is actually a better fit to the azimuths than the BFP. However, the Carlsberg Ridge is opening slowly and lies close to the magnetic equator; the magnetics along this boundary are not of exceptional quality (McKenzie and Sclater, 1971), and we are not disturbed by this slight misfit.

The problem of data inconsistency is evident along the Southeast Indian Ridge. The data are not quite as good along this boundary, but they determine a BFP and angular rate which constitute an acceptable fit (Figure 20). RM1 fits these data very well, but RM2 fits poorly; the RM2 pole is significantly different from the BFP (Figure 6) and does not match the gradient in the spreading rates. The situation is now clear: RM1 satisfies the INDI-AFRC and INDI-ANTA data, but misses badly along the AFRC-ANTA boundary; RM2 corrects the misfit, but then does not satisfy the INDI-ANTA data. The most comprehensive local study of this triple junction was published by McKenzie and Sclater (1971). Their instantaneous motion model is also shown on Figures 18-20. It is different from either RM1 or RM2 but does not constitute a better solution.

The motion of Arabia. In the Gulf of Aden, the rates obtained by Laughton et al. (1970, Table 1) are used directly. These data show very little scatter and are fitted by RM2 very well. The only other data used in the inversions are two rate estimates in the Red Sea (Allan and Morelli, 1970), and these are also well fitted. Because of the mediocre quality of the azimuth data, and the variety of the possible interpretations of Red Sea tectonics (e.g. LePichon et al., 1973), we did not attempt to model the northern Red Sea in this work. Since the Arabian plate is unconstrained along its other boundaries, the RM2 and best-fitting ARAB-AFRC vectors are identical.

The Indian Plate Problem

Although RM2 is a very good fit to the data set as a whole, we have not been able to fit the Indian Ocean data satisfactorily by an RM2-type model. These discrepancies may simply result from bad data, contaminated by systematic observational errors we do not understand. We are aware that data bias is the probable explanation for the misfit to the Aleutian slip vectors; in Paper I, we attributed this misfit, evidently incorrectly, to internal deformation within the North American plate. The existence of systematic errors in the Indian Ocean data obviously cannot be ruled out at this time. However, because its implications are important, an alternate hypothesis--internal deformation within the major plates--deserves investigation.

In RM2, Indian Ocean tectonics are modelled by three plates, ANTA, AFRC and INDI. There is no geological or seismic evidence for deformation within Antarctica; in fact, the intraplate seismicity of Antarctica appears to be the lowest of any major plate (e.g. Tarr, 1974). In contrast, both the African and Indian plates are characterized by high intraplate seismicity, and observations of significant post-Miocene intraplate deformation have been reported (e.g. McKenzie et al., 1970; Sykes, 1970b; Eittreim and Ewing, 1972).

To investigate hypothetical intraplate deformation, we have chopped these plates into two pieces and modelled each as a rigid entity, as we did for NOAM and SOAM. This procedure is obviously unsatisfactory for representing widely distributed strain, and we are implicity assuming that most of the deformation is localized within a relatively narrow zone.

Deformation of the African plate. Active extension across the African Rift valleys is well documented (e.g. McKenzie et al., 1970; Maasha and Molnar, 1972; LePichon et al., 1973). To test the hypothesis that the RM2 misfit along the INDI-ANTA boundary stems from ignoring this deformation, another global inversion was performed. The data along the African plate boundaries in the Red Sea and west of 20°E were assigned to a Nubian plate (NUBI), and the data east of 40°E were assigned to a Somalian plate (SOMA). We arbitrarily assumed that the position of the NUBI-SOMA-ANTA triple junction is somewhere between 20°E and 40°E. Since we did not feel justified in specifying its position more accurately, the 10 data along the Southwest Indian Ridge in this interval were deleted. As expected, the resulting model is a better fit to the data set than RM2. In particular, the INDI-ANTA angular velocity vector is very close to the best-fitting solution in Table 3, and the fit to data along this boundary is much improved. However, the resulting SOMA-NUBI pole is at 43°S, 48°E and the angular rate is 0.17°/My, which implies east-west compressive motion across the African Rift valleys at a rate exceeding 1 cm/yr! This prediction clearly contradicts the geophysical evidence. If a non-zero component of extension is imposed on this boundary, the fit to the INDI-ANTA data set is degraded with respect to RM2.

Therefore, problems with RM2 in the Indian Ocean cannot be remedied by simply postulating internal deformation in Africa, because the resulting model violates other constraints. Although the evidence for extension across the African Rift Zone is compelling, we have not been able to successfully resolve this motion in our global modelling studies, a

ORIGINAL PAGE IS
OF POOR QUALITY

conclusion also stated in Paper I.

In a recent parallel study, Chase (1978) has produced a global plate model which predicts opening of the Rift valleys. The differences between his model and the model described above are evidently due to differences in the inverted data sets. We note that Chase's poles do not provide a satisfactory fit to our data set along the RM2 AFRC-ANTA boundary. Also, the misfit to the INDI-ANTA data set described for RM2 is a feature of his solution as well.

Deformation of the Indian plate. The hypothesis that the Indian plate is deforming is suggested by two aspects of the RM2 fit discussed in the previous pages: RM2's performance is unsatisfactory along both the INDI-ANTA and INDI-PCFC boundaries. To test the hypothesis that INDI deformation is responsible for these discrepancies, the western portion of the Indian plate (WIND) was separated from the eastern portion (AUST). Six INDI-ANTA data within a transition zone between 90°E and 130°E were deleted. Data on the Indian plate boundaries west of 90°E were assigned to WIND and data east of 130° were assigned to AUST. With this configuration, the global data set was inverted. The resulting AUST-WIND angular velocity vector is labelled "A" in Table 4. Again, introduction of more model parameters permits a better fit to the observations: The remaining data along the Southeast Indian Ridge are satisfied, and the AUST-PCFC pole lies within 2° of the INDI-PCFC BFP of Table 3.

From Table 3 we can estimate the hypothetical AUST-WIND VECTOR independently of the data along the Southeast Indian Ridge. Deformation of the Indian plate can be approximately described by the closure vector of the circuit WIND-AFRC-ANTA-PCFC-AUST. This vector may be calculated using the best fitting angular velocity vector for each boundary traversed by the circuit. The result is not unique since the PCFC-AUST rate is not constrained, and a one parameter family of closure vectors is therefore generated. To specify a member of this family, we arbitrarily chose to minimize the relative velocity of AUST with respect to WIND at a point along the Ninetyeast Ridge. Numerical experiments show that the result is quite insensitive to this point's location. The derived angular velocity vector is labelled "B" in Table 4.

In view of the uncertainties involved (and the ad-hoc criterion used to construct vector B), the two solutions in Table 4 are remarkably similar. Both imply slow compressive motion between WIND and AUST in a NW-SE direction.

Our modelling procedures do not require the existence of a specific boundary separating the Indian plate into two portions. However, we speculate that any deformation within the Indian plate may in fact be localized in the vicinity of the Ninetyeast Ridge. This linear feature behaved as an active transform fault in the Cretaceous (eg. McKenzie and Sclater, 1971; Schlich, 1975; Sclater et al., 1976), and, although it has been commonly considered to be quiescent during recent times, Stein and Okal (1977) have suggested that it is now the site of significant seismic and tectonic activity. The nature of this tectonic activity is undoubtedly complex, but Stein and Okal argue that the bottom morphology and seismic source mechanisms are consistent with NW-SE compression in the region, in agreement with the angular velocity vectors in Table 4. Vector A predicts a rate of deformation of about 1 cm/yr, computed at 15°N, 90°E. This rate is equivalent to a strain rate of 10^{-8}/yr, if the deformation were distributed over a zone 1000 km wide, and is grossly compatible with the level of regional seismicity (Stein and Okal, 1977).

In summary, the hypothesis that deformation is occurring within the Indian plate suffices to resolve the difficulties encountered in fitting the instantaneous relative motion data. Although the nature of this deformation remains speculative, at least a partial localization of the deformation in the vicinity of the Ninetyeast Ridge is suggested by other observations. We note that, if extension across the African Rift Zone is incorporated into the plate tectonic model, deformation within the Indian plate predicted by the model will be greater.

Predictions and Implications

Along plate boundaries where data are not available or where interpretation is hindered by geological complications, RM2 provides a useful basis for predictions and comparisons of global motions with local field evidence. We discuss here a few selected examples. In this discussion, prediction errors were calculated using the bilinear form described by Jordan (1975).

Central California. Because of possible bias associated with extension in the Basin and Range Province, data along the San Andreas fault system were not used in the inversion (Figure 1). In central California RM2 predicts a rate of relative motion between the Pacific and North American plates of 5.6 ± 0.3 cm/yr (Table 5). Based on geological evidence, Hall and Sieh (1977) estimate a slip rate of 3.7 ± 0.3 cm/yr along the San Andreas in central California, averaged over three millenia, which is identical to Thatcher's (1977) geodetical estimate of 3.7 ± 0.2 cm/yr. Geological evidence implies a similar rate over the past 10 My (eg. Huffman, 1972). This comparison suggests that a significant fraction of the PCFC-NOAM motion is taken up elsewhere. Some of it may possibly be accommodated on fault systems west of the San Andreas. For example, Weber and Lajoie (1977) conclude that right-lateral slip has occurred along the San Gregorio fault zone during the last 200,000 years, with a rate ranging from 0.6 to 1.3 cm/yr. The discrepancy between the observed and predicted rates may also be attributed to deformation distributed within the Basin and Range Province. Thompson and Burke (1973) estimate that the Basin and Range underwent 100 km of extension in N55W direction during the last 15 My, equivalent to an average of 0.7 cm/yr of right-lateral motion in a direction parallel to the San Andreas.

The comparison of observed and predicted azimuths also suggests active deformation within the western U.S.: Between the Carrizo Plain and Hollister, the San Andreas fault exhibits a well defined azimuth of N41°W ± 2°, whereas the direction of relative motion calculated from RM2 is N35°W ±2° (Table 5). These two values can be reconciled by postulating about 0.8 cm/yr of EW extension between central California and the stable North-American platform to the east. Thompson and Burke's (1973) model implies an average rate for EW Basin and Range extension of 0.5 cm/yr. Furthermore, Clark and Lajoie (1974) estimate a horizontal displacement rate of 0.7 cm/yr along the Garlock Fault during Holocene time. Such agreement may be fortuitous, but we consider it to be support for Davis and Burchfiel's (1973) suggestion that the Garlock Fault is a major intracontinental transform structure.

Relative motion of North and South America. As argued above, relative motion between North and South America is required by our data set. Figure 5 and Table 2 indicate that the NOAM-SOAM vector is poorly constrained and a wide range of possible relative velocities are allowed by the data. Very little direct evidence for this relative motion exists, and the movement could be distributed across a broad zone between, say, 10°N and 20°N. Since the relative velocities are predicted to be small, the deformation may be largely aseismic. However, some seismicity does exist. For example, a magnitude 6.2 earthquake occurred October 23, 1964, at 19.8°N, 56.1°W. The mechanism for this event is consistent with right-lateral strike-slip motion in a direction N55°W (Molnar and Sykes, 1969; J. Dorel, 1975, personal communication), which does not disagree with the RM2 prediction of N71°W ± 58° (Table 5). It is, however, inconsistent with the RM1 model, which predicts left-lateral motion.

Southern Boundary of the Caribbean plate. RM2 predicts a component of NS convergence across the CARB-SOAM boundary. Although the rates are somewhat higher, the azimuths for CARB-SOAM motion are almost identical to those deduced by Jordan (1975) using the RM1 model. Consequently, Jordan's conclusions concerning motions along this boundary are substantiated by this study. They are also supported by Ladd's (1976) model of tertiary plate motions. Direct evidence for NS compressive motion has been obtained by Talwani et al. (1976) from an analysis of multichannel seismic reflection records from the south margin of the Venezuelan Basin and by Rial (1978) from a study of local mechanisms in Columbia and Venezuela. No such compression is predicted by a model which assumes a single American plate. We take this to be an additional argument in favor of modelling NOAM and SOAM as two separate plates with a zone of decoupling between 10°N and 20°N.

Jordan's (1975) portrayal of the tectonic relationships in the Panama Basin is also compatible with RM2. The RM2 COCO-NAZC pole lies north of the equator, and the Panama T.F., as mapped by Lonsdale and Klitgord (1978), closely approximates a small circle about this pole, even though it was not used in the inversion. Thus, RM2 is consistent with the hypothesis that the Panama Basin east of this transform is not acting as a separate plate, as suggested by Molnar and Sykes (1969) and

Lonsdale and Klitgord (1978), but in fact is part of the Nazca plate. Although, RM2 predicts a slightly lower NAZC-CARB rate than RM1, the azimuths of relative motion are nearly identical (Table 5) and are consistent with the hypothesis that the motion is accommodated by a left-lateral transform fault along the southern continental margin of Panama (Jordan, 1975).

Subduction in Southern Chile. Seismic activity along the Chile trench decreases sharply south of the NAZC-ANTA-SOAM triple junction (Tarr, 1974). Few earthquakes (only one with $m_b \geq 6$) have been reported in this region between 1963 and 1975. The predicted convergence rate between ANTA and SOAM is only 2.1 ± 0.2 cm/yr. (Table 5), 6.7 cm/yr less than the subduction velocity north of the triple junction and 30% lower than the RM1 prediction. Yet other convergence zones with comparable rates such as the West Indies Arc or the South Sandwich Trench are significantly more seismically active. If our model is correct, then subduction in Southern Chile takes place largely aseismically, or this boundary constitutes an extensive seismic gap.

The Owen Fracture Zone. The Owen Fracture Zone represents the INDI-ARAB boundary (e.g., McKenzie and Sclater, 1971) and exhibits only weak seismicity. As shown in Table 5, RM2 does predict a low rate of relative motion between these two plates, but the predicted azimuths do not agree well with the observations. At 14°N, Laughton's (1970) bathymetric map indicates an azimuth of N30°E for the Owen fracture zone, compared with the model value of N55°E ± 14°, and at 22°N, a fault plane solution by Sykes (1967) has a slip vector orientation of N50°E, versus a model value

value of N83°E ± 9°. Taken at face value, these data suggest that the INDI-ARAB pole should be translated to the northeast. Interestingly, the inversion with INDI separated into WIND and AUST, described above, yields an WIND-ARAB pole positioned 3° north of the RM2 pole. The azimuth calculated at 14°N, 59°E is N44°N, in better agreement with the observations, although the azimuth calculated at 22°N, 62°E is nearly identical to that for RM2.

Absolute Motions

The RM2 geohedron (Table 2, Figure 2) completely describes the relative motion model. To specify an 'absolute' reference frame, we need only to choose an origin in angular velocity space. A particular frame of interest in discussions of plate dynamics is one fixed with respect to the average position of the deep mantle, assumed to be rigid or at least to have typical internal motions much slower than the motions of the plates; we refer to this frame as the mean mesospheric frame.

In Paper I we constructed an absolute motion model (AM1) based on the Wilson-Morgan fixed hotspot hypothesis and concluded that this hypothesis was consistent with the available instantaneous motion data. However, we noted the difficulties in estimating rates and directions of hotspot migration that are compatible with the short time intervals appropriate to the relative motion model, especially for hotspot traces on the slower plates. Because of these difficulties, we are intrinsically limited in our ability to construct more refined tests of the Wilson-Morgan hypothesis and to discriminate among various instantaneous absolute motion models using hotspot data.

To investigate this limitation, we have derived an absolute motion model by again inverting hotspot data, but restricting the data set to include only those constraints on hotspot migration pertinent to the last 10 My. This time span is really the minimum interval for which good hotspot data can be obtained, although it exceeds by over a factor of three the mean averaging interval for the relative motion data. The azimuths of nine hotspot traces and the rates for five were chosen on the basis of this criterion (Table 6). The data set is dominated by the information from Pacific island chains; no Atlantic or Indian Ocean hotspots were employed. The rate at Hawaii represents our interpretation of the K-Ar ages between Hawaii and French Frigate Shoals summarized by Dalrymple et al. (1974). For four other Pacific archipelagos the K-Ar ages of Duncan et al. (1974) and Duncan and McDougall (1974, 1976) have been used. Azimuth estimates for the traces were obtained from bathymetric charts, and the rate estimates were projected along these directions. The mean rate estimates for individual island chains have formal standard errors of about ± 1 cm/yr (Duncan and McDougall, 1976), but these have been increased to allow for possible errors due to biased sampling. (We note that, since vulcanism may persist at a given site for millions of years, a systematic failure to sample the oldest rocks generally results in rates biased to high values.) The other data in Table 6, hotspot azimuths from the COCO, NAZC and NOAM plates, have been taken from Paper I.

The data set in Table 6 was inverted to obtain an absolute motion model designated AM1-2 (Table 7, Figure 2). In the inversion the relative plate velocity vectors were fixed at their RM2 values, but the uncertainties in the RM2 model, represented by its variance matrix, were incorporated into the calculation of the variance matrix for AM1-2. The model is a very good fit to the selected data set: only one datum has a residual exceeding its assigned error (the azimuth of the Marquesas), and the rate data are all fitted to within 1 cm/yr. Thus, the results of this experiment give us no cause to challenge the Wilson-Morgan hypothesis.

But, even supposing the Wilson-Morgan hypothesis is valid, which we have not proved, with what precision can the motions of the plates in the mean mesospheric frame be predicted by the hotspot data? The answer to this question is indicated by the standard errors of estimation listed in Table 7. Although the absolute velocities of the fast-moving oceanic plates (e.g. PCFC) have relative errors which are small, the relative errors for the slowly-moving continental plates (e.g. EURA) are quite large and in some cases exceed 100%. Hence, the absolute motion directions of several plates, particularly ANTA and EURA, are not usefully constrained by the hotspot data used in this experiment. For example, at the position of Iceland the motion of EURA with respect to the mean mesospheric frame is predicted by AM1-2 to be N83°W at 0.4 cm/yr, nearly diametrically opposed to the direction of the Wyville-Thompson Ridge, the presumed hotspot trace. But no significance should be assigned to this discrepancy, since the formal prediction errors (1σ) are $\pm$ 162° and $\pm$ 0.8 cm/yr, respectively, and since the actual azimuth of the Iceland hotspot trace over the last 10 My is not really known (Paper I, p.566).

With these large uncertainties in mind, it is interesting to compare the hotspot model with absolute motion models based on other criteria. Three such alternate models are listed in Table 8 (see also Figure 2). AM0-2 is the unique absolute motion model constructed by requiring that the lithosphere as a whole possess no net rotation, a criterion discussed and applied in Paper I and by Lliboutry (1974) and Solomon and Sleep (1974). AM2-2 corresponds to Burke and Wilson's (1972) hypothesis that the African plate is stationary with respect to the mantle, a criterion endorsed by Duncan and McDougall (1976) on the basis of Pacific hotspot data. AM3-2 conforms to Jordan's (1975) suggestion that the Caribbean plate is fixed in the mean mesospheric frame, pinned in position by its two bounding subduction zones.

The predictions of these absolute motion models are compared with the selected hotspot data in Table 7. The Pacific poles for all of the absolute motion models are similar (Table 8), and the azimuths of the Pacific island chains are essentially equally well fitted by each. However, the Pacific rate data and the azimuth data from the other plates do provide some discriminants. AM0-2 appears to be inconsistent with the rate data; its values are significantly less than those observed. AM2-2 is a good fit to the Pacific data, but it is a poor fit to the azimuth data for the other three plates. AM2-3 provides a good fit to the azimuth data, but its Pacific rate is slightly low.

The alternative absolute motion models can be compared directly with AM1-2 in model space using the computed estimation errors. Let $\underline{m}$ be the model vector representing AM1-2 and let $\underline{m}'$ be any altenative absolute motion model. Define the quadratic form

$$F = (\underline{m} - \underline{m}')^T \cdot V^{-1} \cdot (\underline{m} - \underline{m}')$$

where V is the complete variance matrix for $\underline{m}$. Then, if $F > (1.96)^2$, $\underline{m}'$ lies outside the AM1-2 95% confidence hyperellipsoid, and one can accept the conclusion that the expected value of $\underline{m}$ (of which $\underline{m}$ is only an estimate) is different from $\underline{m}'$ at the 5% risk level. (Of course, this statement assumes that normal statistics and our linear approximations are applicable and that V is known exactly, which is not strictly true; it nevertheless provides a workable basis for making statistical decisions.) For models AM0-2 and AM2-2, F equals 12.4 and 10.9, respectively; we conclude that these frames are significantly different from the hotspot frame. For AM3-2, F equals only 3.1, so the hypothesis that the Caribbean plate is fixed in the hotspot frame cannot be rejected. We note that the frames corresponding to ANTA fixed ($F = 0.5$) and EURA fixed ($F = 0.8$) are indistinguishable from the hotspot frame as well.

It is also interesting to compare AM1, the absolute motion model derived in Paper I, with AM1-2. Both models were obtained by the inversion of hotspot data, but, in the case of AM1, no rate data were used and a much larger, more globally distributed set of hotspot azimuths were fitted. As a consequence, the averaging intervals for the AM1 data are generally greater than 10 My and more variable. Although the AM1 and AM1-2 Pacific poles are similar, the AM1 rotation rate (0.83 ^{o}/My) is less than that of AM1-2 (0.97 ^{o}/My). For AM1, $F = 339$. This very large value is indicative of the fact that RM1 and RM2 are significantly different relative motion models, in that RM1 lies well outside RM2's 95% confidence hyperellipsoid. A model derived by adding to RM2 the AM1 PCFC absolute rotation vector yields $F = 10.0$ and is inconsistent with the data set in Table 6.

The resolution of absolute motions by the hotspot data is obviously degraded if the possibility of a non-rigid hotspot geometry is allowed. Several authors have concluded that, averaged over geologically long periods of time (> 40 My), hotspots have relative velocities with magnitudes on the order of 1 cm/yr (Morgan, 1972; Burke et al., 1973; Molnar and Atwater, 1973; Molnar and Francheteau, 1975). In some sense, our conservative assignment of large errors to the hotspot data in Table 6 may account for the uncertainties generated by small random motions among the hotspots, but appropriate caution in interpreting any hotspot model must be exercised until better data and more rigorous tests are available.

Nevertheless, several previously published conclusions regarding present-day absolute motions appear to be warranted; these are common to all of the models in Table 8:

(1) Plate speeds correlate negatively with total continental area (Paper I).

(2) Plate speeds correlate positively with the fraction of plate boundary being subducted (Jordan and Minster, 1974; Forsyth and Uyeda, 1975).

(3) Plate speeds correlate positively with geographic co-latitude (Solomon *et al.*, 1975).

Simple mechanical models have been formulated to explain the first two of these correlations (Forsyth and Uyeda, 1975; Solomon *et al.*, 1975; Kaula, 1975), but their true dynamical significance is still quite speculative. For example, Solomon *et al.* (1977) have suggested that these aspects may have very little to do with dynamics; they argue that the absolute plate motions characteristic of Tertiary time exhibit none of the correlations stated above. Although we eye their reconstructions and modelling assumptions with some skepticism (cf. Jurdy, 1977), we agree that more refined tests of the mechanical models must be formulated.

ORIGINAL PAGE IS
OF POOR QUALITY

Perspective

RM2 is a significantly better representation of present-day plate motions than RM1. In a recent parallel study, Chase (1978) has presented a global plate motion model generally quite similar to RM2. Some significant differences between these two models do exist--most ascribable to differences in data selection and interpretation--but the overall agreement is encouraging. These studies should be viewed as ever more rigorous tests of the plate tectonic hypothesis. We continue to be impressed by how well the large data sets (330 members in Table 1) are described by simple models with very few parameters (30 for RM2).

We have noted, however, several problem areas where the plate model does not adequately fit the observations. These discrepancies deserve special scrutiny: they may be the manifestations of tectonic processes or other physical phenomena not now understood. For example, if our hypothesis that the Indian plate is not behaving rigidly is confirmed by better data in the Indian Ocean, then several questions must be addressed. How is the deformation distributed within the plate? What is the nature of the forces driving the deformation? Consider the hypothesis that the deformation is localized in the vicinity of the Ninetyeast Ridge: then a situation exists where, on two opposing plates at approximately equal distances from their common boundary (a spreading center), there are two NS-trending zones of deformation, one extensional (the African Rift) and one compressional (the Ninetyeast Ridge). This unusual configuration should provide a strong discriminant for force-balance models of the sort proposed by Forsyth and Uyeda (1975), Solomon et al. (1975) and Richardson et al. (1976). Of course, more data are required before this hypothetical situation can be accepted as reality.

Throughout the bulk of this paper, the problems of continental tectonics have been carefully avoided. It is clear that, in most regions of intracontinental deformation, the plate model has only limited utility. However, global plate motions do provide the displacement boundary conditions required to understand the kinematics and dynamics of tectonics in complex regions (e.g. Molnar and Taponnier, 1975). These complex regions include not only the continental interiors, but also zones of deformation along the continental margins (e.g. Jordan, 1975) and even boundaries between the oceanic plates themselves. It is possibly complexities of this latter type which are responsible for the difficulties we experienced in obtaining closure about the Azores triple junction.

Unlike the relative motions, the absolute motions of plates in the mean mesospheric frame cannot be precisely constrained. Absolute motion models have been derived from a number of kinematical hypotheses, and, although they are grossly similar, significant differences among them do exist. In our opinion, model AM1-2, with its attendant uncertainties (Table 7), represents the most satisfactory description available from the present observations. Based on these absolute motions, a number of empirical correlations appear to be warranted, but how these correlations relate to the fundamental forces driving the plates is only speculative.

Acknowledgements

We are grateful to Peter Molnar for his contributions during the early stages of this work and to Ken Macdonald and Bill Menard for their comments on the typescript. We thank our many colleagues who allowed us to use their data in advance of publication. This research was sponsored by the National Aeronautics and Space Administration under grant NSG 5089 and by the Division of Geological and Planetary Sciences, California Institute of Technology.

REFERENCES

Abe, K., Mechanisms and tectonic implications of the 1966 and 1970 Peru earthquakes, Phys. Earth Planet. Inter., 5, 367-379, 1972.

Allan, T. D., and C. Morelli, The Red Sea, in The Sea, edited by A. E. Maxwell, Wiley-Interscience, Vol. IV, part 2, pp. 493-542, New York, 1970.

Anderson, R. N., D. W. Forsyth, P. Molnar, and J. Mammerickx, Fault-plane solutions of earthquakes on the Nazca plate boundaries and the Easter plate, Earth Planet. Sci. Lett., 24, 188-202, 1974.

Andrieux, J., J. M. Fontboté, and M. Mattauer, Sur un modèle explicatif de l'arc de Gilbraltar, Earth Planet. Sci. Lett., 12, 191-198, 1971.

ARCYANA, Transform fault and rift valley geology by bathyscaph and diving saucer, Science, 190, 108-116, 1975.

Atwater, T., and K. C. Macdonald, Are spreading centers perpendicular to their transform faults?, Nature, submitted, 1977.

Avery, O. E., Burton, G. D., and J. R. Heirtzler, An aeromagnetic survey of the Norwegian Sea, J. Geophys. Res., 73, 4583-4600, 1968.

Banghar, A. R., and L. R. Sykes, Focal mechanisms in the Indian Ocean and adjacent regions, J. Geophys. Res., 74, 632-649, 1969.

Bergh, H. W., and I. O. Norton, Prince Edward fracture zone and the evolution of the Mozambique basin, J. Geophys. Res., 81, 5221-5239, 1976.

Bird, P., and J. D. Phillips, Oblique spreading near the Oceanographer fracture zone, J. Geophys. Res., 80, 4021-4027, 1975.

Burke, K., and J. T. Wilson, Is the African plate stationary?, Nature, 239, 387-390, 1972.

Burke, K., W. S. F. Kidd, and J. T. Wilson, Relative and latitudinal motion of Atlantic hotspots, Nature, 245, 133-137, 1973.

Chapman, M. E., and S. C. Solomon, North American-Eurasian plate boundary in northeast Asia, J. Geophys. Res., 81, 921-930, 1976.

Chase, C. G., Plate kinematics: The Americas, East Africa, and the rest of the world, Earth Planet. Sci. Lett., in press, 1978.

Choukroune, P., J. Francheteau, and X. Le Pichon, Structural observation in an oceanic transform fault from manned submersibles: Transform fault "A" in the FAMOUS area, Geol. Soc. Amer. Bull., submitted, 1977.

Clark, M. M., and K. R. Lajoie, Holocene behavior of the Garlock fault (abstract), Geol. Soc. Amer. 70th Annual Meeting, Cordilleran section, 6, 156, 1974.

Conant, D. A., Six new focal mechanism solutions for the Arctic and center of rotation for plate movements, M. A. thesis, Columbia University, N. Y., 1972.

Cormier, V. F., Tectonics near the junction of the Aleutian and Kuril-Kamchatka arcs and a mechanism for middle Tertiary magmatism in the Kamchatka basin, Geol. Soc. Amer. Bull., 86, 443-453, 1975.

Dalrymple, G. B., M. A. Lanphere, and E. D. Jackson, Contributions to the petrography and geochronology of volcanic rocks from the Leeward Hawaiian Islands, Geol. Soc. Amer. Bull., 85, 727-738, 1974.

Davis, G. A., and B. C. Burchfiel, Garlock fault: An intracontinental transform structure, Southern California, Geol. Soc. Amer. Bull., 84, 1407-1422, 1973.

Detrick, R., J. D. Mudie, B. P. Luyendyk, and K. C. Macdonald, Near-bottom observations of an active transform fault, Nature, 246, 59-61, 1973.

Dickson, G. O., W. C. Pitman, and J. R. Heirtzler, Magnetic anomalies in the South Atlantic Ocean and ocean floor spreading, J. Geophys. Res., 73, 2087-2100, 1968.

Duncan, R. A., I. McDougall, R. M. Carter, and D. S. Coombs, Pitcairn Island - another Pacific hotspot?, Nature, 251, 679-682, 1974.

Duncan, R. A., and I. McDougall, Migration of volcanism with time in the Marquesas Islands, French Polynesia, Earth Planet. Sci. Lett., 21, 414-420, 1974.

Duncan, R. A., and I. McDougall, Linear volcanism in French Polynesia, J. Volcan. Geotherm. Res. 1, 197-227, 1976.

Eittreim, S. L., and J. Ewing, Mid-plate tectonics in the Indian Ocean, J. Geophys. Res., 77, 6413-6421, 1972.

Eittreim, S. L., and J. Ewing, Vema fracture zone transform fault, Geology, 3, 555-558, 1975.

Engdahl, E. R., N. H. Sleep, and Ming-Te Lin, Plate effects in North-Pacific subduction zones, Tectonophysics, 95-116, 1977.

Engel, C. G., and R. L. Fisher, Granitic to ultramafic rock complexes of the Indian Ocean ridge system, western Indian Ocean, Geol. Soc. Amer. Bull., 86, 1553-1578, 1975.

Falconer, R. H. K., The Indian-Antarctic-Pacific triple junction, Earth Planet. Sci. Lett., 17, 151-158, 1972.

Falconer, R. K. H., Indian-Pacific rotation pole determined from earthquake epicenters, Nature Phys. Sci., 243, 97-99, 1973.

Fisher, R. L., J. G. Sclater, and D. P. McKenzie, The evolution of the Central Indian Ridge, western Indian Ocean, Geol. Soc. Amer. Bull., 82, 553-562, 1971.

Forsyth, D. W., Mechanisms of earthquakes and plate motions in the East Pacific, Earth Planet. Sci. Lett., 17, 189-193, 1972.

Forsyth, D. W., Fault plane solutions and tectonics of the South Atlantic and Scotia Sea, J. Geophys. Res., 80, 1429-1443, 1975.

Forsyth, D. W., and S. Uyeda, On the relative importance of driving forces of plate motion, Geophys. J. R. Astr. Soc., 43 163-200, 1975.

Fox, P. S., W. C. Pitman, and F. Shephard, Crustal plates in the central Atlantic: Evidence for at least two poles of rotation, Science, 165, 487-489, 1969.

Fox, P. J., F. W. Schroeder, R. M. Moody, W. C. Pitman, and P. J. Hoose, The bathymetry of the Oceanographer fracture zone and the Mid-Atlantic Ridge at 35°N with implications for central north Atlantic plate motion, Deep Sea Res., submitted, 1977.

Fukao, Y., Thrust faulting at a lithospheric plate boundary--the Portugal earthquake of 1969, Earth Planet. Sci. Lett., 18, 205-216, 1973.

Hadley, D., and H. Kanamori, Seismotectonics of the eastern Azores-Gibraltar ridge (abstract), Eos, Trans. Amer. Geophys. Union, 56, 1028, 1975.

Hall, N. T., and K. E. Sieh, Late Holocene rate of slip on the San Andreas fault in the northern Carrizo Plain, San Luis Obispo County, California (abstract), Geol. Soc. Amer. 73rd Annual Meeting, Cordilleran section, 9, 428, 1977.

Hayes, D. E., and J. R. Connolly, Morphology of the Southeast Indian Ocean, Antarctic Oceanology II: The Australian-New Zealand Sector, edited by D. E. Hayes, Amer. Geophys. Union, Washington, D. C., pp. 125-146, 1972.

Heezen, B. C., and M. Tharp, Tectonic fabric of the Atlantic and Indian Oceans and continental drift, Phil. Trans. R. Soc. Lond. Ser. A., 258, 90-106, 1965.

Heirtzler, J. R., G. O. Dickson, E. M. Herron, W. C. Pitman, and X. Le Pichon, Marine magnetic anomalies, geomagnetic field reversals and motions of the sea floor and continents, J. Geophys. Res., 73, 2119-2136, 1968.

Herron, E.M., Sea-floor spreading and the Cenozoic history of the east-central Pacific, Geol. Soc. Amer. Bull., 83, 1671-1672, 1972.

Herron, E. M., and D. E. Hayes, A geophysical study of the Chile ridge, Earth Planet. Sci. Lett., 6, 77-83, 1969.

Hey, R. N., Tectonic evolution of the Cocos-Nazca Rise, Ph.D. thesis, Princeton Univ., Princeton, N. J., 1974.

Hodgson, J. H., and W. G. Milne, Direction of faulting in certain earthquakes of the North Pacific, Bull. Seismol. Soc. Amer., 41, 221-242, 1951.

Holcombe, T. L., P. R. Vogt, J. E. Matthews, and R. R. Murchison, Evidence for sea-floor spreading in the Cayman Trough, Earth Planet. Sci. Lett., 20, 357-371, 1973.

Isacks, B., L. R. Sykes, and J. Oliver, Focal mechanisms of deep and shallow earthquakes in the Tonga-Kermadec region and the tectonics of island arcs, Geol. Soc. Amer. Bull., 80, 1143-1470, 1969.

Johnson, G. L., J. R. Southall, P. W. Young, and P. R. Vogt, Origin and structure of the Iceland plateau and Kolbeinsey ridge, J. Geophys. Res., 77, 5688-5696, 1972.

Johnson, T., and P. Molnar, Focal mechanisms and plate tectonics of the Southwest Pacific, J. Geophys. Res., 77, 5000-5032, 1972.

Jordan, T. H., The present-day motions of the Caribbean plate, J. Geophys. Res., 80, 4433-4439, 1975.

Jordan, T. H., and J. B. Minster, Plate motions with respect to the mantle (abstract), Eos, Trans. Amer. Geophys. Union, 55, 557, 1974.

Jordan, T. H., J. B. Minster, and P. Molnar, Present-day plate motions (abstract), Eos, Trans. Amer. Geophys. Union, 57, 329, 1976.

Jurdy, D. M., An alternate model for absolute plate motions in the early Tertiary (abstract), Eos, Trans. Amer. Geophys. Union, 58, 503, 1977.

Kanamori, H., and G. S. Stewart, Seismological aspects of the Guatemala earthquake of February 4, 1976, preprint.

Kaula, W. M., Absolute plate motions by boundary velocity minimizations, J. Geophys. Res., 80, 244-248, 1975.

Klitgord, K. D., and J. D. Mudie, The Galapagos Spreading Centre: A near-bottom geophysical survey, Geophys. J. R. Astr. Soc., 38, 563-586, 1974.

Klitgord, K. D., J. D. Mudie, J. Grow, and P. A. Larson, Fast sea-floor spreading on the Chile ridge, Earth Planet. Sci. Lett. 20, 93-99, 1973.

Krause, C. C., and N. D. Watkins, North-Atlantic crustal genesis in the vicinity of the Azores, Geophys. J. R. Astr. Soc., 19, 261-284, 1970.

Ladd, J. W., Relative motion of South America with respect to North America and Caribbean tectonics, Geol. Soc. Amer. Bull., 87, 969-976, 1976.

Larson, R. L., and C. G. Chase, Relative velocities of the Pacific, North American and Cocos plates in the Middle America region, Earth Planet. Sci. Lett., 7, 425-428, 1970.

Laughton, A. S., A new bathymetric chart of the Red Sea, Phil. Trans. R. Soc. Lond. Ser. A., 267, 21-22, 1970.

Laughton, A. S., R. B. Whitmarsh, J. S. M. Rusby, M. L. Somers, J. Revie, B. S. McCartney, and J. E. Nafe, A continuous east-west fault of the Azores-Gilbraltar Ridge, Nature, 327, 217-220, 1972.

Laughton, A. S., D. G. Roberts, and R. Graves, Bathymetry of the northeast Atlantic: Mid-Atlantic Ridge to southwest Europe, Deep Sea Res., 22, 791-810, 1975.

Laughton, A. S., R. B. Whitmarsh, and M. T. Jones, The evolution of the Gulf of Aden, Phil. Trans. R. Soc. Lond. Ser. A., 267, 227-266, 1970.

Lawver, L. A., J. W. Hawkins, and J. G. Sclater, Magnetic anomalies and crustal dilation in the Lau Basin, Earth Planet. Sci. Lett., 33, 27-35, 1976.

Le Pichon, X., J. Francheteau, and J. Bonnin, Plate Tectonics, 300 pp., Elsevier, New York, 1973.

Lliboutry, L., Plate movement relative to rigid lower mantle, Nature, 250, 298-300, 1974.

Lonsdale, P., Regional shape and tectonics of the equatorial East Pacific Rise, Mar. Geophys. Res., in press, 1977.

Lonsdale, P., Near-bottom reconnaissance of a fast-slipping transform fault at the Pacific-Nazca plate boundary, J. Geol., in press, 1978.

Lonsdale, P., and K. D. Klitgord, Structure and tectonic history of the eastern Panama basin, Geol. Soc. Amer. Bull., in press, 1978.

Maasha, N., and P. Molnar, Earthquake fault parameters and tectonics in Africa, J. Geophys. Res., 77, 5731-5743, 1972.

Macdonald, K. C., Near-bottom magnetic anomalies, asymmetric spreading, oblique spreading, and tectonics of the Mid-Atlantic Ridge near lat. 37°N, Geol. Soc. Amer. Bull., 88, 541-555, 1977.

Macdonald, K. C., and T. L. Holcombe, Inversion of magnetic anomalies and sea-floor spreading in the Cayman Trough, Tectonophysics, submitted, 1978.

Macdonald, K., and B. P. Luyendyk, Deep-tow studies of the structure of the Mid-Atlantic Ridge crest near 37°N (FAMOUS), Geol. Soc. Amer. Bull., 88, 621-636, 1977.

Mammerickx, J., R. N. Anderson, H. W. Menard, and S. M. Smith, Morphology and tectonic evolution of the East-Central Pacific, Geol. Soc. Amer. Bull., 86, 111-118, 1975.

McGregor, B. A., C. G. A. Harrison, J. W. Lavelle, and P. A. Rona, Magnetic anomaly patterns on Mid-Atlantic Ridge Crest at 26°N, J. Geophys. Res., 82, 231-238, 1977.

McKenzie, D., Active tectonics of the Mediterranean region, Geophys. J. R. Astr. Soc., 30, 109-185, 1972.

McKenzie, D. P., D. Davies, and P. Molnar, Plate tectonics of the Red Sea and East Africa, Nature, 226, 1-6, 1970.

McKenzie, D. P., and R. L. Parker, Plate tectonics in ω space, Earth Planet. Sci. Lett., 22, 285-293, 1974.

McKenzie, D. P., and J. G. Sclater, The evolution of the Indian Ocean since the late Cretaceous, Geophys. J. R. Astr. Soc., 25, 437-528, 1971.

Menard, H. W., and T. Atwater, Origin of fracture-zone topography, Nature, 22, 1037-1040, 1969.

Minster, J. B., and T. H. Jordan, Modelling present-day motions (abstract), Eos, Trans. Amer. Geophys. Union, 58, 367, 1977.

Minster, J. B., T. H. Jordan, P. Molnar, and E. Haines, Numerical modelling of instantaneous plate tectonics, Geophys. J. R. Astr. Soc., 36, 541-576, 1974.

Minster, J. F., J. B. Minster, M. Treuil, and C. J. Allègre, Systematic use of trace elements in igneous processes, part II. Inverse problem of the fractional crystallization process, Contrib. Mineral. Petrol., 61, 49-77, 1977.

Molnar, P., Fault plane solutions of earthquakes and direction of motion in the Gulf of California and on the Rivera fracture zone, Geol. Soc. Amer. Bull. 84, 1651-1658, 1973.

Molnar, P., and T. Atwater, Relative motion of hot spots in the mantle, Nature, 246, 541-576, 1974.

Molnar, P., T. Atwater, J. Mammerickx, and S. M. Smith, Magnetic anomalies, bathymetry, and the tectonic evolution of the South Pacific since the late Cretaceous, Geophys. J. R. Astr. Soc., 40, 383-420, 1975.

Molnar, P., and J. Francheteau, The relative motion of "hot spots" in the Atlantic and Indian oceans during the Cenozoic, Geophys. J. R. Astr. Soc., 43, 763-774, 1975.

Molnar, P., and L. R. Sykes, Tectonics of the Caribbean and Middle America regions from focal mechanisms and seismicity, Geol. Soc. Amer. Bull., 80, 1639-1684, 1969.

Molnar, P., and P. Tapponnier, Cenozoic tectonics of Asia: Effects of a continental collision, Science, 189, 419-426, 1975.

Morgan, W. J., Plate motions and deep mantle convection, Geol. Soc. Amer. Memoir 132, 7-22, 1972.

ORIGINAL PAGE IS
OF POOR QUALITY

Morgan, W. J., P. R. Vogt, and D. E. Falls, Magnetic anomalies and sea-floor spreading on the Chile Rise, Nature, 222, 137-142, 1968.

Norton, I. O., The present relative motion between Africa and Antarctica, Earth Planet. Sci. Lett., 33, 219-230, 1976.

Olivet, J. L., X. Le Pichon, S. Monti, and B. Sichler, Charlie-Gibbs fracture zone, J. Geophys. Res., 79, 2059-2972, 1974.

Phillips, J. D., Magnetic anomalies over the Mid-Atlantic Ridge near 27°N, Science, 157, 920-923, 1967.

Pitman, W. C., E. M. Herron, and J. R. Heirtzler, Magnetic anomalies in the Pacific and sea-floor spreading, J. Geophys. Res., 73, 2069-2085, 1968.

Pitman, W. C., and M. Talwani, Sea-floor spreading in the North Atlantic Geol. Soc. Amer. Bull., 83, 619-646, 1972.

Rea, D. L., Changes in the axial configuration of the East Pacific Rise near 6°S during the last 2 M. y., J. Geophys. Res., 81 1495-1504, 1976a.

Rea, D. K., Analysis of a fast-spreading rise crest: The East Pacific Rise, 9° to 12° South, Mar. Geophys. Res., 2, 291-313, 1976b.

Rea, D. K., and R. J. Blakely, Short wavelength magnetic anomalies in a region of rapid sea-floor spreading, Nature, 255, 126-128, 1975.

Rial, J. A., The Caracas, Venezuela, earthquake of July 1967: a multiple source event, J. Geophys. Res., in press, 1978 .

Richardson, R. M., S. C. Solomon, and N. H. Sleep, Intraplate stresses as an indicator of plate tectonic driving forces, J. Geophys. Res., 81, 1847-1856, 1976.

Rosendahl, B. R., Preliminary site survey report: IPOD Survey Area PT-4, Scripps Institution of Oceanography, La Jolla, California, 1976.

Rusnack, G. A., R. L. Fisher, and F. P. Shephard, Bathymetry and faults of Gulf of California, Marine Geology of California, Memoir 3, edited by Tj. H. Van Andel, and G. G. Shor, Jr., Amer. Assoc. Petrol. Geol., Tulsa, Oklahoma, pp. 59-75, 1964.

Schlich, R., Structure et age de l'océan indien occidental, Mémoire hors série N°6, 102 pp., Société Géologique de France, 1975.

Schlich, R., and P. Patriat, Mise en évidence d'anomalies magnétiques axiales sur la branche ouest de la dorsale médio-indienne, C. R. Acad. Sci., Paris, 272, 700-703, 1971.

Sclater, J. G., R. N. Anderson, M. L. Bell, Elevation of ridges and evolution of the Central East Pacific, J. Geophys. Res., 76, 7888-7915, 1971.

Sclater, J. G., C. Bowin, R. Hey, H. Hoskins, J. Peirce, J. Phillips, and C. Tapscott, The Bouvet triple junction, J. Geophys. Res., 81, 1857-1869, 1976.

Sclater, J. G., B. P. Luyendyk, and L. Meinke, Magnetic lineations in the southern part of the Central Indian Basin, Geol. Soc. Amer. Bull., 87, 371-378, 1976.

Solomon, S. C., Shear-wave attenuation and melting beneath the Mid-Atlantic Ridge, J. Geophys. Res., 78, 6044-6059, 1973.

Solomon, S. C., and N. H. Sleep, Some simple physical models for absolute plate motions, J. Geophys. Res., 79, 2557-2567, 1974.

Solomon, S. C., N. H. Sleep, and D. M. Jurdy, Mechanical models for absolute plate motions in the early Tertiary, J. Geophys. Res., 82, 203-212, 1977.

Solomon, S. C., N. H. Sleep, and R. M. Richardson, On the forces driving plate tectonics: inferences from absolute plate velocities and intraplate stress, Geophys. J. R. Astr. Soc., 42, 769-802, 1975.

Stauder, W., The Alaska earthquake of July 20, 1958: Seismic studies, Bull. Seismol. Soc. Amer., 50, 293-322, 1960.

Stauder, W., Mechanism of the Rat Island earthquake sequence of February 4, 1965, with relation to island arcs and sea-floor spreading, J. Geophys. Res., 73, 3847-3858, 1968a.

Stauder, W., Tensional character of earthquake foci beneath the Aleutians, J. Geophys. Res., 73, 7693-7701, 1968b.

Stauder, W., Mechanism and spatial distribution of Chilean earthquakes with relation to subduction of the oceanic plate, J. Geophys. Res., 78, 5033-5061, 1973.

Stauder, W., Subduction of the Nazca plate under Peru as evidenced by focal mechanisms and by seismicity, J. Geophys. Res., 80, 1053-1064, 1975.

Stauder, W., and G. A. Bollinger, The focal mechanism of the Alaska earthquake and its aftershocks, J. Geophys. Res., 71, 5283-5296, 1966.

Stauder, W., and L. Mualchin, Fault motion in the larger earthquakes of the Kuril-Kamchatka arc and of the Kuril-Hokkaido corner, J. Geophys. Res., 81, 297-308, 1976.

Stein, S., H. J. Melosh, and J. B. Minster, Ridge migration and asymmetric sea-floor spreading, Earth Planet. Sci. Lett., 36, 51-62, 1977.

Stein, S., and E. A. Okal, Seismicity and tectonics of the Ninetyeast Ridge area: Evidence for internal deformation of the Indian plate, J. Geophys. Res., submitted, 1977.

Sykes, L. R., Mechanism of earthquakes and nature of faulting on the mid-ocean ridges, J. Geophys. Res., 72, 2131-2153, 1967.

Sykes, L. R., Focal mechanism solutions for earthquakes along the world rift system, Bull. Seismol. Soc. Amer. 60, 1749-1752, 1970a.

Sykes, L. R., Seismicity of the Indian Ocean and a possible nascent island arc between Ceylon and Australia, J. Geophys. Res., 75, 5041-5055, 1970b.

Talwani, M., C. C. Windisch, P. L. Stoffa, P. Buhl, and R. E. Houtz, Multi-channel seismic study in the Venezuelan basin and the Curacao Ridge (abstract), Eos, Trans. Amer. Geophys. Union, 57, 266, 1976.

Talwani, M., C. C. Windisch, and M. G. Langseth, Reykjanes ridge crest: a detailed geophysical study, J. Geophys. Res., 76, 473-517, 1971.

Tarr, A. C., World seismicity map, U. S. Geological Survey, 1974.

Thatcher, W., Secular deformation, episodic movements, and relative plate motions in Southern California (abstract), Eos, Trans. Amer. Geophys. Union, 58, 496, 1977.

Thompson, G. A., and D. B. Burke, Rate and direction of spreading in Dixie Valley, Basin and Range Province, Nevada, Geol. Soc. Amer. Bull., 84, 627-632, 1973.

Tobin, D. G., and L. R. Sykes, Seismicity and tectonics of the northeast Pacific Ocean, J. Geophys. Res., 73, 3821-3845, 1968.

Uchupi, E., Eastern Yucatan continental margin and western Caribbean tectonics, Amer. Assoc. Petrol. Geol. Bull., 57, 1075-1085, 1973.

Udías, A., A. López Arroyo, and J. Mezcua, Seismotectonic of the Azores-Alboran region, Tectonophysics, 31, 259-289, 1976.

Van Andel, Tj. H., D. K. Rea, R. P. Von Herzen, and H. Hoskins, Ascension fracture zone, Ascension Island, and the Mid-Atlantic Ridge, Geol. Soc. Amer. Bull., 84, 1527-1546, 1973.

Vogt, P. R., N. A. Ostenso, and G. L. Johnson, Magnetic and bathymetric data bearing on sea-floor spreading north of Iceland, J. Geophys. Res., 75, 903-920, 1970.

Weber, G. E., and K. R. Lajoie, Late Pleistocene and Holocene tectonics of the San Gregorio fault zone between Moss Beach and Point Ano Nuevo, San Mateo County, California (abstract), Geol. Soc. Amer. 73rd Annual Meeting, Cordilleran section, 9, 524, 1977.

Weissel, J. K., and D. E. Hayes, Magnetic anomalies in the south-east Indian Ocean, Antarctic Oceanology II: The Australian-New Zealand Sector, edited by D. E. Hayes, Amer. Geophys. Union, Washington, D.C., pp. 165-196, 1972.

Weissel, J. K., and D. E. Hayes, The Australian-Antarctic discordance: new results and implications, J. Geophys. Res., 79, 2579-2587, 1974.

Appendix

In the interpretation of earthquake mechanisms along subduction boundaries, most authors assume that the direction of relative plate motion is given by the horizontal projection of the slip vector (e.g. Paper I). If the convergence is oblique to the trench axis, this procedure yields a biased estimate of the direction of relative motion. Instead, the slip vector should be rotated into the horizontal plane, which requires correcting the slip vector azimuth by an amount α given by

$$\alpha = \operatorname{arccot}\left(\frac{\cot(T_A - T_F)}{\sin P_F}\right) + T_F - T_A$$

where T_F, P_F, and T_A, P_A are the azimuth and plunge of the poles of the fault plane and auxiliary plane, respectively.

This correction was applied to the data from the Aleutian-Kuril, South American and Tonga-Kermadec Trenches. The statistical information is summarized below:

	$\lvert\bar{\alpha}\rvert$	$\bar{\alpha}$	$\lvert\alpha\ \max\rvert$
NOAM-PCFC	0.6°	0.3°	2°
NAZC-SOAM	0.9°	0°	2°
PCFC-INDI	1.1°	-0.9°	4°

This correction is clearly minor. Thus, as pointed out by Chase (1978), omitting this correction does not give rise to a significant systematic bias in the data.

Table 1. The RM2 data set.*

ORIGINAL PAGE IS OF POOR QUALITY

	LAT.N	LON.E	DATUM	S.D.	MODEL	RESID.	IMP.	REFERENCE
				**** PCFC NOAM ****				
RA	23.40	-108.50	5.60	0.40	5.73	0.07	0.403	LARSON & CHASE (1970)
TF	24.10	-105.00	N50W	10.0	N51W	-0.9	0.040	MUSNACK ET AL.(1964)
	25.00	-109.60	N50W	5.0	N50W	0.2	0.142	"
	26.80	-111.10	N53W	10.0	N47W	5.4	0.040	"
	29.30	-113.80	N45W	5.0	N44W	0.9	0.157	"
SV	23.10	-107.90	N55W	10.0	N52W	2.7	0.040	MOLNAR (1973)
	25.30	-109.20	N45W	10.0	N50W	-4.8	0.041	"
	26.20	-110.40	N45W	15.0	N48W	-3.6	0.018	"
	26.30	-110.20	N49W	10.0	N48W	0.6	0.041	SYKES (1970 A)
	28.50	-112.10	N42W	15.0	N45W	-3.4	0.018	MOLNAR (1973)
	29.70	-113.70	N45W	10.0	N44W	1.3	0.040	SYKES (1970 A)
	31.70	-114.60	N51W	10.0	N41W	9.7	0.040	"
	50.80	-130.00	N15W	15.0	N19W	-4.2	0.015	TOBIN & SYKES (1968)
	54.10	-132.60	N26W	10.0	N16W	9.8	0.034	HODGSON & MILNE (1951)
	58.30	-136.90	N22W	10.0	N13W	8.5	0.034	STAUDER (1960)
	61.05	-147.50	N24W	10.0	N18W	6.3	0.029	STAUDER & BOLLINGER (1966)
	56.60	-152.20	N27W	10.0	N25W	1.9	0.024	"
	56.40	-152.90	N23W	10.0	N26W	-2.5	0.024	"
	56.50	-154.40	N25W	10.0	N27W	-1.5	0.023	"
	55.70	-155.60	N24W	10.0	N28W	-4.0	0.023	"
	53.10	-167.60	N31W	20.0	N36W	-4.4	0.005	STAUDER (1968 B)
	51.40	179.10	N39W	20.0	N45W	-5.5	0.004	STAUDER (1968 A)
	52.10	175.70	N37W	20.0	N46W	-9.2	0.004	"
	51.90	174.60	N28W	20.0	N47W	-18.8	0.004	"
	52.30	174.30	N29W	20.0	N47W	-17.9	0.004	"
	53.03	171.11	N34W	20.0	N48W	-14.5	0.004	CORMIER (1976)
	54.28	160.23	N45W	20.0	N50W	-4.8	0.004	"
	57.80	163.50	N60W	10.0	N52W	8.4	0.017	STAUDER & MUALCHIN (1976)
	56.00	163.30	N59W	10.0	N52W	6.7	0.017	"
	49.20	156.10	N50W	10.0	N58W	-8.1	0.015	"
	47.20	153.80	N54W	10.0	N60W	-5.8	0.015	"
	47.10	153.60	N58W	10.0	N60W	-1.9	0.015	"
	46.50	153.20	N61W	10.0	N60W	0.8	0.015	"
	45.60	150.90	N60W	10.0	N62W	-1.6	0.014	"
	44.90	150.10	N59W	10.0	N62W	-3.2	0.014	"
	44.90	149.50	N60W	10.0	N63W	-2.5	0.014	"
	44.70	150.70	N49W	10.0	N62W	-12.6	0.014	"
	44.60	150.30	N60W	10.0	N62W	-2.1	0.014	"
	44.30	149.50	N58W	10.0	N63W	-4.6	0.014	"
	44.00	148.10	N59W	10.0	N63W	-4.4	0.014	"
	43.90	148.70	N59W	10.0	N63W	-4.1	0.014	"
	43.60	148.00	N59W	10.0	N64W	-4.5	0.014	"
				**** COCO PCFC ****				
RA	17.30	-105.40	8.90	0.40	8.99	-0.09	0.139	SCLATER ET AL.(1971)
	16.70	-105.70	9.20	0.40	9.24	-0.04	0.133	"
	16.00	-105.20	9.40	0.40	9.51	-0.11	0.126	"
	14.90	-104.30	10.10	0.40	9.98	0.12	0.120	"
	14.10	-104.00	10.40	0.40	10.30	0.10	0.116	"
	12.80	-104.00	10.80	0.40	10.80	0.00	0.113	"
	12.50	-104.00	11.00	0.40	10.91	0.09	0.113	HERRON (1972)
	11.00	-103.80	11.50	0.40	11.49	0.01	0.117	SCLATER ET AL.(1971)
TF	16.00	-105.00	N80E	10.0	N85E	5.2	0.037	LARSON & CHASE (1970)
	8.40	-103.50	N84E	3.0	N84E	0.0	0.235	ROSENDAHL (1976)
SV	8.50	-103.00	N76E	15.0	N83E	7.2	0.009	MOLNAR & SYKES (1969)
				**** COCO NOAM ****				
SV	17.30	-100.10	N44E	15.0	N37E	-7.3	0.032	MOLNAR & SYKES (1969)
	16.30	-95.80	N36E	10.0	N35E	-1.4	0.051	"
	16.00	-97.90	N40E	10.0	N37E	-3.1	0.059	"
	15.90	-96.20	N37E	15.0	N34E	-3.5	0.023	"
				**** COCO CARB ****				
SV	12.90	-87.40	N34E	15.0	N27E	-7.4	0.030	MOLNAR & SYKES (1969)
	11.40	-86.20	N32E	10.0	N28E	-4.4	0.060	"
	8.90	-83.40	N30E	15.0	N29E	-0.5	0.021	"
				**** CARB NOAM ****				
RA	18.00	-81.50	2.00	0.40	1.94	0.06	0.952	MACDONALD & HOLCOMBE (1978)
TF	16.40	-87.00	N72E	3.0	N73E	0.7	0.412	UCHUPI (1973)
	16.90	-85.00	N75E	3.0	N75E	-0.2	0.272	"
	17.50	-83.00	N79E	3.0	N77E	-2.1	0.188	HOLCOMBE ET AL.(1973)
	19.20	-80.00	N79E	3.0	N80E	1.2	0.172	"
	19.70	-77.00	N83E	3.0	N83E	0.3	0.281	"
	19.70	-75.00	N86E	3.0	N85E	-0.7	0.416	"
SV	15.27	-89.25	N66E	10.0	N70E	4.2	0.060	KANAMORI & STEWART (1977)
	16.80	-85.90	N70E	20.0	N74E	3.9	0.007	MOLNAR & SYKES (1969)
	18.90	-81.20	N81E	15.0	N79E	-2.1	0.006	"
	19.10	-64.80	S82E	15.0	S84E	-2.1	0.074	"
	17.70	-61.60	N90E	15.0	S81E	9.3	0.106	"
				**** COCO NAZC ****				
RA	2.30	-99.60	4.40	0.30	4.56	-0.16	0.280	HEY (1974)
	2.40	-98.70	4.90	0.30	4.71	0.19	0.249	"
	2.30	-96.00	5.00	0.30	5.16	-0.16	0.160	"
	2.50	-94.00	5.50	0.30	5.48	0.02	0.120	"
	2.40	-93.00	5.60	0.30	5.64	-0.04	0.107	"
	0.90	-87.00	6.40	0.40	6.60	-0.20	0.077	"
	0.80	-86.10	6.60	0.30	6.73	-0.13	0.157	"
	0.80	-86.09	7.00	0.20	6.73	0.27	0.355	KLITGORD & MUDIE (1974)
	0.80	-81.00	6.20	0.40	6.75	-0.55	0.090	HEY (1974)
	3.10	-83.20	7.20	0.30	7.11	0.09	0.217	"
TF	1.40	-85.30	N 5E	5.0	N 7E	2.2	0.200	LONSDALE & KLITGORD (1978)
	2.50	-84.50	N 6E	3.0	N 6E	-0.2	0.532	"
SV	2.00	-90.30	N 1W	10.0	N 7E	8.1	0.064	FORSYTH (1972)
	1.50	-85.30	N 0E	20.0	N 7E	7.1	0.012	MOLNAR & SYKES (1969)

Table 1 (continued).

	LAT.N	LON.E	DATUM	S.D.	MODEL	RESID.	IMP.	REFERENCE
				**** NAZC PCFC ****				
RA	-5.80	-106.80	15.30	0.80	15.43	-0.13	0.071	REA (1976 A)
	-9.40	-110.00	16.30	0.40	15.93	0.37	0.073	REA (1976 B)
	-9.90	-110.10	15.50	0.40	15.98	-0.48	0.074	"
	-10.80	-110.30	16.60	1.00	16.08	0.52	0.048	"
	-11.40	-110.50	16.10	1.00	16.14	-0.04	0.049	"
	-12.00	-110.90	15.90	0.40	16.21	-0.31	0.130	"
	-19.00	-113.00	16.55	1.00	16.78	-0.24	0.064	HERRON (1972)
	-20.00	-113.90	16.10	0.60	16.84	-0.74	0.197	REA & BLAKELY (1975)
	-28.00	-112.00	17.50	0.80	17.10	-0.40	0.145	HERRON (1972)
TF	-3.70	-102.90	S81E	3.0	S81E	0.3	0.138	LONSDALE (1978)
	-4.50	-105.50	S78E	3.0	S79E	-1.2	0.141	LONSDALE (1977)
	-6.00	-107.00	S73E	5.0	S78E	-5.5	0.350	HAMMERICKX ET AL.(1975)
	-13.50	-112.00	S70E	10.0	S76E	-6.4	0.012	"
SV	-4.40	-105.90	S75E	20.0	S79E	-4.0	0.003	ANDERSON ET AL.(1974)
	-4.50	-106.50	S76E	15.0	S79E	-2.9	0.006	ANDERSON & SCLATER (1972)
	-4.40	-105.80	S77E	15.0	S79E	-2.0	0.006	"
	-13.30	-111.50	S75E	30.0	S77E	-1.7	0.003	"
	-20.60	-114.10	S75E	15.0	S76E	-0.9	0.005	ANDERSON ET AL.(1974)
	-24.90	-113.40	S71E	10.0	S76E	-5.2	0.011	"
	-28.70	-112.70	S62E	20.0	S77E	-14.6	0.003	"
				**** NAZC SOAM ****				
SV	-6.90	-80.40	N73E	15.0	N82E	9.0	0.021	STAUDER (1975)
	-10.70	-78.60	N60E	10.0	N81E	21.3	0.045	ABE (1972)
	-14.90	-75.50	N89E	15.0	N80E	-8.9	0.020	STAUDER (1975)
	-21.80	-70.00	N86E	10.0	N77E	-8.5	0.047	STAUDER (1973)
	-23.10	-70.10	N74E	10.0	N78E	3.6	0.046	"
	-24.10	-70.30	N81E	15.0	N78E	-3.3	0.020	"
	-25.50	-70.70	N89E	15.0	N78E	-11.4	0.018	"
	-27.90	-70.90	N73E	10.0	N78E	5.3	0.344	"
	-30.00	-71.50	S80E	20.0	N78E	-21.7	0.011	"
	-30.60	-71.40	N87E	20.0	N78E	-8.8	0.011	"
	-30.60	-71.50	N79E	20.0	N78E	-0.7	0.011	"
	-30.70	-71.20	N73E	15.0	N78E	5.1	0.019	"
	-31.50	-71.00	N82E	15.0	N78E	-4.0	0.019	"
	-33.50	-71.90	N85E	20.0	N78E	-9.5	0.011	"
	-34.00	-72.20	N74E	20.0	N79E	4.6	0.011	"
	-37.80	-73.40	N81E	15.0	N79E	-1.9	0.018	"
	-38.10	-73.40	S79E	20.0	N79E	-21.9	0.010	"
	-38.10	-73.00	N80E	10.0	N79E	-1.1	0.042	"
	-38.20	-73.20	N81E	15.0	N79E	-2.0	0.018	"
	-38.50	-73.50	N70E	20.0	N79E	9.1	0.010	"
	-46.30	-74.80	N87E	20.0	N79E	-7.5	0.011	"
				**** NAZC ANTA ****				
RA	-40.50	-92.00	7.60	0.80	6.69	0.91	0.246	KLITGORD ET AL.(1973)
TF	-41.30	[illegible]	N80E	10.0	N85E	5.2	0.054	KLITGORD ET AL.(1973)
SV	-36.20	-100.90	N82E	10.0	S86E	12.4	0.061	ANDERSON ET AL.(1974)
	-36.30	-97.20	N79E	20.0	S88E	12.6	0.015	"
	-36.40	-97.20	N89E	15.0	S88E	2.6	0.026	"
	-36.50	-97.50	S87E	10.0	S88E	-1.2	0.060	"
	-41.70	-84.00	N86E	10.0	N82E	-4.0	0.050	"
				**** PCFC ANTA ****				
RA	-35.40	-110.90	10.60	0.40	10.44	0.16	0.111	HERRON (1972)
	-35.80	-110.90	10.30	0.40	10.43	-0.13	0.110	MOLNAR ET AL.(1975)
	-36.00	-111.00	10.20	0.50	10.42	-0.22	0.070	"
	-42.00	-111.20	9.90	0.40	10.11	-0.21	0.095	"
	-44.40	-112.70	10.00	0.40	9.94	0.06	0.039	"
	-47.60	-112.90	9.80	0.40	9.70	0.10	0.054	"
	-51.40	-118.10	9.50	0.50	9.31	0.19	0.050	"
	-53.70	-118.00	9.83	0.50	9.10	0.73	0.049	"
	-54.50	-118.70	8.80	0.50	9.01	-0.21	0.049	"
	-55.20	-121.20	9.10	0.50	8.90	0.20	0.049	"
	-56.50	-138.20	8.80	0.50	8.54	0.26	0.050	"
	-56.00	-145.00	8.40	0.50	8.17	0.23	0.052	"
	-58.50	-149.00	8.00	0.50	7.76	0.24	0.055	"
	-59.60	-151.30	7.70	0.60	7.56	0.14	0.040	"
	-60.50	-151.00	7.80	0.50	7.47	0.33	0.056	PITMAN ET AL.(1968)
	-63.20	-163.10	6.00	0.70	6.67	-0.67	0.035	MOLNAR ET AL.(1975)
	-64.10	-169.00	5.60	0.50	6.30	-0.70	0.073	"
	-65.00	-174.00	5.80	0.50	5.96	-0.16	0.078	PITMAN ET AL.(1968)
TF	-49.80	-115.00	N72W	5.0	N74W	-2.0	0.036	MOLNAR ET AL.(1975)
	-53.00	-118.50	N70W	5.0	N72W	-1.9	0.036	"
	-54.50	-119.00	N65W	5.0	N71W	-3.4	0.040	"
	-55.20	-125.00	N68W	3.0	N69W	-0.5	0.110	"
	-55.50	-130.00	N67W	3.0	N66W	0.8	0.110	"
	-56.20	-143.00	N60W	3.0	N60W	-0.2	0.113	"
	-59.80	-150.50	N63W	5.0	N55W	7.8	0.047	"
	-64.50	-170.50	N48W	5.0	N42W	5.9	0.039	"
	-64.90	175.20	N34W	3.0	N35W	-1.2	0.247	"
SV	-56.00	-123.40	N67W	10.0	N69W	-2.0	0.010	MOLNAR ET AL.(1975)
	-54.80	-136.00	N61W	10.0	N64W	-2.8	0.010	"
	-56.60	-142.50	N61W	10.0	N60W	0.7	0.010	"
	-65.70	-179.30	N51W	15.0	N36W	14.7	0.009	"
				**** PCFC INDI ****				
SV	-24.70	-176.90	N58W	10.0	N53W	5.5	0.022	ISACKS ET AL.(1969)
	-29.80	-177.20	N70W	10.0	N82W	-11.9	0.029	"
	-29.90	-177.80	N76W	20.0	N82W	-6.5	0.007	"
	-29.90	-177.70	N86W	20.0	N82W	3.6	0.007	"
	-30.10	-177.70	N73W	10.0	N82W	-8.9	0.029	"
	-30.20	-177.80	S88W	20.0	N82W	9.6	0.037	"
	-30.50	-178.10	N88W	20.0	N83W	5.4	0.038	JOHNSON & MOLNAR (1972)
	-30.70	-178.30	N78W	15.0	N83W	-4.8	0.014	"
	-30.70	-178.30	N79W	15.0	N83W	-4.4	0.014	"
	-30.90	-177.60	N90W	20.0	N82W	7.9	0.008	"
	-32.20	-178.10	N90W	20.0	N83W	7.8	0.004	"
	-33.50	-179.00	S72W	20.0	N83W	15.2	0.004	"
	-49.00	163.70	S90W	25.0	S67W	10.9	0.024	BANGHAR & SYKES (1969)
	-56.20	158.20	S 0E	20.0	S35W	35.0	0.059	"

ORIGINAL PAGE IS OF POOR QUALITY

Table 1 (continued).

	LAT.N	LON.E	DATUM	S.D.	MODEL	RESID.	IMP.	REFERENCE
			**** EURA NOAM ****					
RA	72.10	1.00	1.60	0.40	1.59	0.01	0.171	VOGT ET AL.(1970)
	70.00	-15.00	1.80	0.30	1.73	0.07	0.239	"
	61.60	-27.00	1.90	0.30	2.01	-0.11	0.168	TALWANI ET AL.(1971)
	61.00	-28.00	2.00	0.30	2.03	-0.03	0.163	"
	60.00	-29.40	2.00	0.30	2.06	-0.06	0.156	"
	46.00	-27.50	2.70	0.50	2.36	0.34	0.043	PITMAN & TALWANI (1972)
	46.00	-28.50	2.80	0.50	2.40	0.40	0.045	"
	40.00	-30.00	2.80	0.50	2.46	0.34	0.050	KRAUSE & WATKINS (1970)
TF	79.00	2.50	S52E	10.0	S54E	-2.0	0.069	JOHNSON ET AL.(1972)
	71.00	-8.00	S65E	5.0	S66E	-1.4	0.204	"
	64.50	-20.00	S82E	10.0	S75E	7.2	0.037	AVERY ET AL.(1968)
	52.50	-33.50	S85E	3.0	S83E	1.5	0.316	OLIVET ET AL.(1974)
SV	79.80	2.60	S43E	10.0	S53E	-10.2	0.071	CONANT(1972)
	79.80	2.40	S47E	10.0	S53E	-6.3	0.070	"
	80.20	-1.00	S52E	10.0	S56E	-3.5	0.070	"
	70.90	-7.60	S65E	10.0	S66E	-1.2	0.051	"
	66.70	-18.20	S65E	10.0	S74E	-8.8	0.038	"
	66.30	-19.80	S73E	10.0	S75E	-1.7	0.037	SYKES (1967)
	52.80	-34.30	S85E	10.0	S84E	1.2	0.029	SOLOMON (1973)
			**** AFRC EURA ****					
TF	37.00	-22.00	S84W	5.0	S86W	2.4	0.783	LAUGHTON ET AL.(1975)
SV	37.50	-24.70	S82W	15.0	S75W	-6.7	0.145	MCKENZIE (1972)
	37.60	-24.70	S89W	20.0	S75W	-13.6	0.079	UDIAS ET AL.(1976)
	37.40	-19.00	S83W	20.0	N81W	16.3	0.065	"
	35.90	-17.40	N63W	20.0	N73W	-9.9	0.140	HADLEY & KANAMORI (1975)
	36.10	-10.60	N42W	15.0	N47W	-5.2	0.565	UDIAS ET AL.(1976)
	36.20	-7.60	N39W	25.0	N40W	-0.5	0.193	MCKENZIE (1972)
			**** AFRC NOAM ****					
RA	36.80	-33.30	2.20	0.30	2.31	-0.11	0.166	MACDONALD (1977)
	36.00	-34.00	2.40	0.30	2.34	0.06	0.165	BIRD & PHILLIPS (1975)
	27.50	-44.30	2.50	0.30	2.59	-0.09	0.190	PHILLIPS (1967)
	26.20	-44.80	2.40	0.30	2.62	-0.22	0.200	MCGREGOR ET AL.(1977)
	22.50	-45.00	2.80	0.40	2.69	0.11	0.110	PHILLIPS (1967)
TF	34.90	-33.10	S88E	10.0	S78E	9.9	0.053	MACDONALD & LUYENDYK (1977)
	34.60	-33.40	S89E	10.0	S79E	10.9	0.053	"
	23.90	-46.00	S84E	10.0	S80E	4.1	0.073	FOX ET AL.(1969)
	15.50	-46.80	S85E	10.0	S80E	4.7	0.067	HEEZEN & THARP (1965)
SV	35.30	-36.10	N90E	10.0	S78E	11.6	0.059	UDIAS ET AL.(1976)
	23.90	-46.00	S76E	15.0	S80E	-3.9	0.032	SYKES (1967)
			**** AFRC SOAM ****					
RA	-6.00	-11.70	3.50	0.40	3.62	-0.12	0.115	VAN ANDEL ET AL.(1973)
	-7.60	-13.40	3.80	0.40	3.84	-0.04	0.113	"
	-8.40	-13.30	3.80	0.40	3.86	-0.06	0.110	"
	-9.20	-13.20	3.90	0.40	3.87	0.03	0.108	"
	-24.90	-13.00	4.50	0.40	3.95	0.55	0.076	DICKSON ET AL.(1968)
	-28.30	-13.00	3.90	0.40	3.93	-0.03	0.072	"
	-32.50	-14.00	4.00	0.20	3.91	0.09	0.278	"
	-37.20	-13.00	4.00	0.50	3.80	0.20	0.042	"
	-54.20	-1.30	3.10	0.30	3.29	-0.19	0.142	SCLATER ET AL.(1976)
	-54.70	-1.00	3.20	0.30	3.27	-0.07	0.144	"
TF	10.80	-42.30	S88E	2.0	S88E	0.4	0.506	EITTREIM & EWING (1975)
	10.20	-40.90	S86E	5.0	S88E	-2.3	0.075	HEEZEN & THARP (1965)
	9.40	-40.00	S88E	5.0	S89E	-0.7	0.070	"
	8.80	-38.70	S88E	10.0	S89E	-1.3	0.016	"
	7.63	-36.60	S89E	10.0	N90E	-1.3	0.015	"
	7.20	-34.30	S89E	10.0	N89E	-2.4	0.014	"
	4.00	-31.50	N85E	10.0	N88E	-3.4	0.012	"
	1.90	-30.60	N88E	10.0	N87E	1.1	0.012	"
	1.10	-26.00	N86E	10.0	N85E	-0.9	0.012	"
	-0.10	-16.00	N77E	5.0	N82E	4.9	0.062	"
	-1.10	-24.00	N81E	10.0	N84E	3.4	0.012	"
	-1.35	-14.50	N75E	3.0	N81E	5.5	0.194	"
	-1.90	-12.90	N82E	10.0	N80E	-2.0	0.019	"
	-2.90	-12.50	N73E	10.0	N80E	6.9	0.018	"
	-7.00	-12.50	N79E	5.0	N80E	1.1	0.069	VAN ANDEL ET AL.(1973)
SV	10.80	-43.30	N90E	10.0	S87E	2.9	0.021	SYKES (1967)
	-0.20	-18.70	N89E	10.0	N83E	-5.9	0.015	"
	-0.50	-19.90	N85E	10.0	N83E	-2.4	0.014	"
	-54.30	-2.40	N66E	10.0	N74E	8.1	0.022	FORSYTH (1975)
			**** ANTA SOAM ****					
RA	-55.30	-1.70	2.00	0.40	1.94	0.06	0.082	SCLATER ET AL.(1976)
	-56.10	-4.70	1.90	0.40	1.90	0.00	0.089	"
TF	-55.70	-3.00	S84E	3.0	S84E	-2.0	0.408	SCLATER ET AL.(1976)
SV	-55.50	-2.60	S85E	10.0	S84E	1.9	0.055	FORSYTH (1975)
	-58.30	-15.30	N90E	15.0	S86E	4.4	0.026	"
	-60.80	-24.60	S74E	10.0	S85E	-11.3	0.084	"
	-60.60	-25.70	S73E	10.0	S85E	-12.3	0.096	"
	-60.40	-19.70	S82E	15.0	S85E	-3.3	0.032	"
			**** AFRC ANTA ****					
RA	-54.70	0.0	1.60	0.40	1.58	0.02	0.082	SCLATER ET AL.(1976)
	-53.90	3.50	1.40	0.40	1.59	-0.19	0.081	"
	-52.20	14.90	1.70	0.30	1.62	0.08	0.112	NORTON (1977)
	-44.20	38.40	1.60	0.70	1.65	-0.05	0.268	BERGH & NORTON (1976)
	-44.10	39.00	1.60	0.40	1.65	-0.05	0.067	SCHLICH & PATRIAT (1971)
	-38.80	47.30	1.60	0.30	1.65	-0.05	0.125	"
TF	-54.90	1.80	N44E	5.0	N45E	0.9	0.181	SCLATER ET AL.(1976)
	-52.20	14.00	N36E	5.0	N34E	-7.5	0.124	NORTON (1977)
	-46.00	33.20	N17E	3.0	N16E	-1.0	0.234	BERGH & NORTON (1976)
	-44.00	34.00	N14E	5.0	N14E	-2.1	0.086	"
	-43.70	34.70	N17E	5.0	N13E	-4.0	0.087	"
	-30.00	60.90	N 1E	3.0	N 2E	1.1	0.531	ENGEL & FISHER (1975)

ORIGINAL PAGE IS
OF POOR QUALITY

Table 1 (continued).

	LAT.N	LON.E	DATUM	S.D.	MODEL	RESID.	IMP.	REFERENCE
			**** AFRC ANTA ****					
SV	-54.60	1.70	N47E	10.0	N43E	-1.9	0.046	FORSYTH (1975)
	-54.40	5.90	N40E	10.0	N41E	1.1	0.041	"
	-53.90	8.70	N47E	10.0	N39E	-4.5	0.037	NORTON (1977)
	-50.90	29.10	N26E	15.0	N21E	-5.1	0.010	"
	-48.80	31.50	N17E	20.0	N19E	1.9	0.005	SYKES (1970)
	-45.60	34.10	N17E	15.0	N17E	-0.2	0.009	NORTON (1977)
	-45.40	35.00	N16E	15.0	N14E	0.1	0.009	"
	-45.50	35.10	N15E	15.0	N16E	1.0	0.009	"
	-44.90	35.70	N25E	15.0	N16E	-9.4	0.009	"
	-38.90	46.20	N14E	15.0	N 9E	-5.3	0.012	"
	-36.20	52.50	N 5E	20.0	N 5E	0.2	0.008	"
			**** INDI AFRC ****					
MA	7.90	59.10	2.40	0.40	1.95	0.45	0.107	MCKENZIE & SCLATER (1971)
	6.80	60.00	2.70	0.40	2.12	0.55	0.105	"
	5.10	61.60	2.70	0.40	2.39	0.31	0.100	"
	4.10	62.40	2.80	0.30	2.56	0.24	0.173	"
	-20.30	66.50	4.90	0.40	4.85	0.05	0.071	"
	-21.50	68.50	4.90	0.40	5.03	-0.13	0.072	"
	-21.80	68.70	5.00	0.40	5.06	-0.06	0.072	"
	-22.00	68.90	4.90	0.40	5.08	-0.18	0.072	"
	-24.30	70.00	5.20	0.40	5.30	-0.10	0.073	"
TF	11.00	57.50	N30E	5.0	N31E	0.7	0.420	LAUGHTON (1970)
	0.50	67.00	N43E	5.0	N40E	-2.8	0.090	FISHER ET AL.(1971)
	-5.50	68.50	N45E	5.0	N46E	1.1	0.064	"
	-9.00	67.30	N52E	3.0	N51E	-0.7	0.165	ENGEL & FISHER (1975)
	-13.50	66.50	N57E	3.0	N56E	-0.9	0.153	"
	-16.00	66.50	N60E	5.0	N58E	-2.1	0.052	FISHER ET AL.(1971)
	-17.60	66.20	N62E	3.0	N59E	-2.9	0.142	ENGEL & FISHER (1975)
	-20.00	67.00	N60E	10.0	N60E	-0.4	0.012	FISHER ET AL.(1971)
			**** INDI ANTA ****					
MA	-28.00	74.00	6.10	0.50	6.58	-0.48	0.052	MCKENZIE & SCLATER (1971)
	-29.50	75.00	6.10	0.40	6.68	-0.58	0.050	SCLATER ET AL.(1976)
	-41.00	79.00	6.80	0.30	7.18	-0.38	0.143	SCHLICH (1975)
	-41.00	81.00	7.30	0.60	7.22	0.08	0.036	MCKENZIE & SCLATER (1971)
	-42.00	90.00	7.40	0.60	7.38	0.02	0.038	"
	-44.00	93.00	7.20	0.40	7.44	-0.24	0.059	"
	-50.00	114.00	7.50	0.40	7.40	0.10	0.114	WEISSEL & HAYES (1972)
	-50.50	134.00	7.40	0.40	6.97	0.43	0.143	"
	-62.50	157.80	6.50	0.40	6.32	0.18	0.159	FALCONER (1972)
	-62.40	158.10	6.60	0.40	6.31	0.49	0.159	"
TF	-39.50	78.50	N42E	15.0	N45E	2.5	0.007	MCKENZIE & SCLATER (1971)
	-36.50	79.00	N46E	15.0	N43E	-4.6	0.037	"
	-39.50	80.50	N39E	15.0	N43E	3.9	0.007	"
	-43.00	84.50	N34E	15.0	N40E	5.4	0.236	"
	-46.00	96.00	N29E	15.0	N32E	3.0	0.006	"
	-49.60	124.00	N13E	5.0	N12E	-1.4	0.055	WEISSEL & HAYES (1974)
	-58.00	149.00	N19W	10.0	N12W	6.7	0.018	HAYES & CONNOLLY (1972)
	-60.00	153.00	N19W	10.0	N17W	1.6	0.019	"
	-61.80	159.00	N26W	15.0	N20W	5.8	0.009	FALCONER (1972)
SV	-45.80	96.10	N17E	10.0	N32E	14.9	0.013	BANGHAR & SYKES (1969)
	-55.20	146.10	N13W	15.0	N 8W	4.8	0.008	"
	-55.30	146.20	N22W	25.0	N 8W	13.6	0.003	"
			**** ARAB AFRC ****					
MA	14.30	59.00	1.60	0.40	1.51	0.09	0.162	ALLAN & MORELLI (1970)
	18.00	40.00	1.60	0.40	1.58	0.02	0.128	"
	14.80	54.80	2.12	0.20	2.12	0.00	0.037	LAUGHTON ET AL.(1970)
	14.70	55.60	2.20	0.20	2.14	0.06	0.108	"
	14.60	56.00	2.26	0.20	2.15	0.11	0.121	"
	14.40	53.40	2.06	0.20	2.09	-0.03	0.067	"
	14.30	52.50	2.20	0.20	2.17	0.03	0.141	"
	13.70	57.30	2.22	0.20	2.21	0.01	0.152	"
	12.40	50.70	1.96	0.10	2.02	-0.06	0.181	"
	13.20	50.90	2.00	0.10	2.03	-0.03	0.186	"
	12.10	45.80	1.90	0.10	1.89	0.01	0.309	"
	12.00	45.60	1.92	0.10	1.89	0.03	0.319	"
TF	13.50	51.50	N30E	5.0	N30E	0.4	0.698	LAUGHTON ET AL.(1970)
	12.00	44.00	N35E	10.0	N34E	-1.4	0.216	"
SV	14.00	51.70	N30E	15.0	N30E	-0.1	0.077	SYKES (1970 B)

*For rates (MA), units are cm/yr; for transform fault (TF) and slip vector (SV) azimuths, units are degrees.

Table 2. RM2 Geohedron

Plate Pair	Relative Rotation Vector*						Error Ellipse**			Importance Distribution			
	θ ($^\circ$N)	σ_θ (deg)	ϕ ($^\circ$E)	σ_ϕ (deg)	ω ($^\circ$/My)	σ_ω ($^\circ$/My)	ζ_{max} (deg)	σ_{max} (deg)	σ_{min} (deg)	MA	TF	SV	Total
NOAM-PCFC	48.77	1.10	-73.91	1.94	0.852	0.025	S71E	1.30	1.08	0.405	0.398	0.694	1.497
COCO-PCFC	38.72	0.89	-107.39	1.01	2.208	0.070	S37E	1.00	0.63	0.977	0.272	0.009	1.258
NAZC-PCFC	56.64	1.89	-87.88	1.81	1.539	0.029	N09E	1.91	0.96	0.849	0.341	0.038	1.228
EURA-PCFC	60.64	1.04	-78.92	3.04	0.977	0.027	S78E	1.51	1.02	0	0	0	0
INDI-PCFC	60.71	0.77	-5.79	1.83	1.246	0.023	S82E	0.90	0.76	0	0	0.246	0.246
ANTA-PCFC	64.67	0.90	-80.23	2.32	0.964	0.014	N52E	1.11	0.75	1.200	0.811	0.039	2.050
COCO-NOAM	29.80	1.06	-121.28	2.07	1.489	0.070	S75E	1.84	0.99	0	0	0.165	0.165
AFRC-NOAM	80.43	1.57	56.36	35.29	0.258	0.019	N86E	5.88	1.51	0.851	0.246	0.091	1.188
EURA-NOAM	65.85	6.17	132.44	5.06	0.231	0.015	S14E	6.36	1.39	1.055	0.626	0.366	2.047
NOAM-CARB	-33.83	9.19	-70.48	2.76	0.219	0.052	S13E	9.42	0.97	0.952	1.741	0.253	2.946
COCO-CARB	23.60	1.48	-115.55	2.26	1.543	0.084	S63E	2.24	1.21	0	0	0.111	0.111
NAZC-CARB	47.30	5.37	-97.57	4.57	0.711	0.056	S19E	5.59	2.67	0	0	0	0
COCO-NAZC	5.63	1.40	-124.40	2.61	0.972	0.065	N89E	2.60	1.40	1.829	0.732	0.076	2.637
NOAM-SOAM	25.57	7.12	-53.82	6.22	0.167	0.029	S14E	7.22	5.49	0	0	0	0
CARB-SOAM	73.51	11.75	-60.84	48.86	0.202	0.038	S52E	16.84	6.84	0	0	0	0
NAZC-SOAM	59.08	3.76	-94.75	3.73	0.835	0.034	S05E	3.77	1.90	0	0	0.464	0.464
AFRC-SOAM	66.56	2.83	-37.29	2.65	0.356	0.010	S08E	2.85	0.99	1.201	1.108	0.072	2.381
ANTA-SOAM	87.69	1.30	75.20	79.29	0.302	0.018	N84E	3.22	1.26	0.167	0.608	0.283	1.058
INDI-AFRC	17.27	0.97	46.02	1.06	0.644	0.014	S47E	1.24	0.66	0.843	1.098	0	1.941
ARAB-AFRC	30.82	3.44	6.43	11.48	0.260	0.047	S79E	10.02	2.93	1.989	0.934	0.077	3.000
AFRC-EURA	25.23	4.25	-21.19	0.98	0.104	0.036	S01E	4.25	0.89	0	0.783	1.167	1.950
INDI-EURA	19.71	1.40	38.46	2.66	0.698	0.024	S65E	2.72	0.90	0	0	0	0
ARAB-EURA	29.82	2.53	-1.64	9.57	0.357	0.054	S85E	8.33	2.45	0	0	0	0
INDI-ARAB	7.08	2.15	63.86	2.30	0.469	0.066	S51E	2.51	1.89	0	0	0	0
NAZC-ANTA	43.21	4.50	-95.02	3.28	0.605	0.039	S01E	4.50	2.39	0.246	0.058	0.222	0.526
AFRC-ANTA	9.46	3.77	-41.70	3.55	0.149	0.009	S42E	4.93	1.45	0.697	1.243	0.195	2.135
INDI-ANTA	18.67	1.16	32.74	1.41	0.673	0.011	S62E	1.39	1.10	1.012	0.135	0.025	1.172
									Totals	14.273	11.134	4.593	30.000

*First plate named moves counterclockwise with respect to the second. Uncertainties are the standard deviations of marginal distributions.

**One sigma error ellipses are specified by the azimuth of the major axis ζ_{max}; lengths of the axes are geocentric angles.

Table 3. Best-fitting angular velocity vectors for individual plate boundaries.*

Plate Pair	Relative Rotation Vector						Error Ellipse			Importance Distribution			
	θ ($^\circ$N)	σ_θ (deg)	ϕ ($^\circ$E)	σ_ϕ (deg)	ω ($^\circ$/My)	σ_ω ($^\circ$/My)	ζ_{max} (deg)	σ_{max} (deg)	σ_{min} (deg)	MA	TF	SV	Total
NOAM-PCFC	49.02	1.34	-76.05	2.82	0.885	0.071	N86E	1.85	1.34	1.000	0.615	1.385	3.000
COCO-PCFC	37.68	3.39	-107.74	1.84	2.298	0.317	S10E	3.44	1.35	2.002	0.965	0.033	3.000
NAZC-PCFC	55.64	6.72	-85.76	5.40	1.527	0.062	N22E	7.20	1.62	1.978	0.928	0.094	3.000
INDI-PCFC	55.71	2.75	-5.00	3.42	—	—	S19E	2.84	1.79	0	0	2.000	2.000
[illegible]	65.39	1.55	-79.26	3.40	0.976	0.022	N41E	1.92	0.85	1.800	1.150	0.050	3.000
[illegible]	[illegible]	16.51	-17.69	60.61	0.275	[illegible]	[illegible]	17.91	3.38	1.706	0.977	0.317	3.000
[illegible]	[illegible]	9.72	127.37	9.83	0.252	[illegible]	[illegible]	[illegible]	[illegible]	[illegible]	0.772	[illegible]	[illegible]
NOAM-CARB	-34.18	9.28	-70.40	2.80	0.225	[illegible]	[illegible]	[illegible]	[illegible]	[illegible]	[illegible]	[illegible]	[illegible]
COCO-NAZC	4.90	1.54	-123.65	2.71	0.993	0.071	S69E	2.70	1.54	2.003	0.903	[illegible]	[illegible]
AFRC-SOAM	62.98	3.46	-39.14	2.46	0.357	0.010	S06E	3.48	1.07	1.407	1.491	0.102	3.000
INDI-AFRC	19.63	1.78	44.12	1.81	0.612	0.035	S44E	2.34	0.76	1.682	1.318	0	3.000
ARAB-AFRC	30.82	3.44	6.43	11.48	0.260	0.047	S79E	10.02	2.93	1.989	0.934	0.077	3.000
AFRC-EURA	25.71	4.07	-21.04	0.95	—	—	S01E	4.07	0.85	0	0.793	1.207	2.000
AFRC-ANTA	7.93	4.98	-38.72	4.77	0.146	0.011	S43E	6.70	1.51	1.038	1.666	0.296	3.000
INDI-ANTA	11.85	2.76	34.74	2.99	0.672	0.013	N65E	2.98	2.71	2.008	0.839	0.153	3.000

*Symbols and conventions the same as Table 2.

ORIGINAL PAGE IS
OF POOR QUALITY

Table 4. Hypothetical AUST-WIND rotation vectors described in text.

	θ °N	φ °E	ω °/My
A	-45.90	36.95	0.134
B	-38.04	15.26	0.130

Table 5. RM2-predicted plate motions at selected points

Plate Pair	Lat. (°N)	Long. (°E)	Rate cm/yr.	Azimuth
PCFC-NOAM	36.4	-121.0	5.6 ± 0.3	N35W ± 2.
NOAM-SOAM	20.0	-56.0	0.2 ± 0.3	N71W ± 58.
	15.0	-60.0	0.4 ± 0.3	N62W ± 31.
SOAM-CARB	10.0	-66.0	2.3 ± 0.5	N77W ± 10.
	10.0	-74.0	2.2 ± 0.5	N78W ± 10.
NAZC-CARB	7.5	-79.0	5.4 ± 0.5	N71E ± 5.
ANTA-SOAM	-50.0	-75.0	2.1 ± 0.2	S88E ± 5.
ARAB-INDI	22.0	62.0	1.4 ± 0.2	N83E ± 9.
	14.0	59.0	0.8 ± 0.2	N55E ± 14.

Table 6. A comparison between hotspot data and absolute motion models.

Hotspot	Lat. (°N)	Long. (°E)	Trace	Plate	Observed Azimuth (deg)	Observed Rate (cm/yr)	AM1-2 Azimuth (deg)	AM1-2 Rate (cm/yr)	Importance Distribution Azimuths	Importance Distribution Rates	AM0-2 Azimuth (deg)	AM0-2 Rate (cm/yr)	AM2-2 Azimuth (deg)	AM2-2 Rate (cm/yr)	AM3-2 Azimuth (deg)	AM3-2 Rate (cm/yr)
Hawaii	20	-155	Hawaiian Islands	PCFC	N64W ± 10	10.0 ± 2.0	N60W	9.7	0.292	0.141	N61W	7.7	N57W	10.9	N62W	8.8
Marquesas	-11	-138	Marquesas Islands	PCFC	N45W ± 15	9.8 ± 2.0	N67W	10.7	0.078	0.200	N65W	8.2	N62W	11.6	N67W	9.5
Tahiti-Mehetia	-18	-148	Society Islands	PCFC	N65W ± 15	11.0 ± 2.0	N64W	10.7	0.084	0.225	N63W	8.0	N60W	11.5	N65W	9.4
Macdonald	-29	-140	Austral Islands	PCFC	N55W ± 15	10.5 ± 2.0	N66W	10.5	0.074	0.239	N63W	7.8	N60W	11.2	N65W	9.1
Pitcairn	-25	-130	Pitcairn-Gambier	PCFC	N65W ± 15	11.0 ± 3.0	N70W	10.7	0.065	0.099	N66W	8.1	N64W	11.5	N68W	9.4
Juan de Fuca	46	-130	Cobb Seamounts	PCFC	N54W ± 15	-	N47W	5.5	0.389	-	N49W	5.0	N43W	7.0	N50W	5.4
Galapagos	-1	-92	Cocos Ridge	[illegible]	N45E ± 10	-	N46E	8.5	0.174	-	N52E	10.6	N38E	9.2	N49E	9.5
Galapagos	-1	-92	Carnegie Ridge	NAZC	S85E ± 10	-	N88E	4.9	0.480	-	N83E	7.2	N71E	4.7	N85E	5.9
Yellowstone	45	-110	Snake River Plain	NOAM	S60W ± 20	-	S56W	2.4	0.460	-	S55W	2.1	N87W	2.3	S58W	2.4

ORIGINAL PAGE IS
OF POOR QUALITY

Table 7. Model AM1-2

Plate	Absolute Rotation Vector: θ (^oN)	σ_θ (deg)	ϕ (^oE)	σ_ϕ (deg)	ω (^{o}/My)	σ_ω (^{o}/My)	Error Ellipse: ζ_{max} (deg)	σ_{max} (deg)	σ_{min} (deg)
AFRC	18.76	33.93	-21.76	42.20	0.139	0.055	S73E	40.40	33.24
ANTA	21.85	91.81	75.55	63.20	0.054	0.091	N12E	93.01	56.12
ARAB	27.29	12.40	-3.94	18.22	0.388	0.067	S76E	16.38	12.11
CARB	-42.80	39.20	66.75	40.98	0.129	0.104	N30E	43.21	23.90
COCO	21.89	3.08	-115.71	2.81	1.422	0.119	S32E	3.35	2.25
EURA	0.70	124.35	-23.19	146.67	0.038	0.057	S67E	151.10	118.90
INDI	19.23	6.96	35.64	6.57	0.716	0.076	S25E	7.16	5.97
NAZC	47.99	9.36	-93.81	9.14	0.585	0.097	S02E	9.37	5.43
NOAM	-58.31	16.21	-40.67	39.62	0.247	0.080	S57E	23.12	12.14
PCFC	-61.66	5.11	97.19	7.71	0.967	0.085	S16E	5.23	3.50
SOAM	-82.28	19.27	75.67	85.88	0.285	0.084	N03E	19.28	11.38

Table 8. Absolute motion models.

Model	Kinematical Condition	Pacific Rotation Vector: Lat. (^oN)	Long. (^oE)	Rate (^{o}/My)
AM0-2	No net rotation	-62.93	111.50	0.736
AM1-2	Best fit to hotspot data	-61.66	97.19	0.967
AM2-2	African plate fixed	-59.15	109.60	1.043
AM3-2	Caribbean plate fixed	-63.52	104.45	0.853

Figure Captions

Figure 1. Plate geometry and geographical distribution of the data used in producing model RM2. Circles indicate seafloor-spreading rates, squares represent transform faults, and triangles slip vectors. Seven EURA-NOAM data at high latitudes are not shown on the figure.

Figure 2. RM2 geohedron (stereo pair). The geohedron depicts relative motions in angular velocity space (McKenzie and Parker, 1974). Individual plates correspond to vertices. The z axis coincides with the rotation axis of the earth, the x axis is along the Greenwich meridian. Vectors representing the three reference axes have a magnitude of 0.3°/My. Open circle is coordinate origin for AM0-2. Closed circle is coordinate origin for AM1-2.

Figure 3. Histograms of normalized residuals for each data type, with sample size, sample mean and sample variance. The theoretically ideal Gaussian distributions with zero mean and unit variance are shown for comparison. Shaded area in lower histograms represents residuals for Aleutian and Kuril slip vectors, which show negative bias.

Figure 4. Poles for model RM2, with their 95 percent (2σ) confidence ellipses. RM1 poles and best fitting poles where available (BFP, Table 3) are also shown.

Figure 5. See Figure 4.

Figure 6. See Figure 5

Figure 7. In Figures 7 - 20, data and models are shown as residuals with respect to the predicted values calculated from the best fitting angular velocity vectors. Azimuths are measured in degrees in a counterclockwise direction, rates are in centimeters per year. Data symbols are the same as in Figure 1. Error bars are the subjective error bars listed in Table 1. The solid lines represent model RM2 (this study) and the dashed lines represent model RM1 (Paper I). Here the dashed-dotted line corresponds to the Bering-Pacific pole determined in Paper I.

Figure 8. See Figure 7.

Figure 9. See Figure 7.

Figure 10. See Figure 7.

Figure 11. See Figure 7.

Figure 12. See Figure 7.

ORIGINAL PAGE IS
OF POOR QUALITY

Figure 13. See Figure 7.

Figure 14. See Figure 7.

Figure 15. See Figure 7.

Figure 16. See Figure 7.

Figure 17. See Figure 7.

Figure 18. See Figure 7. The dotted line represents the instantaneous motion model of McKenzie and Sclater (1971).

Figure 19. See Figure 18.

Figure 20. See Figure 18.

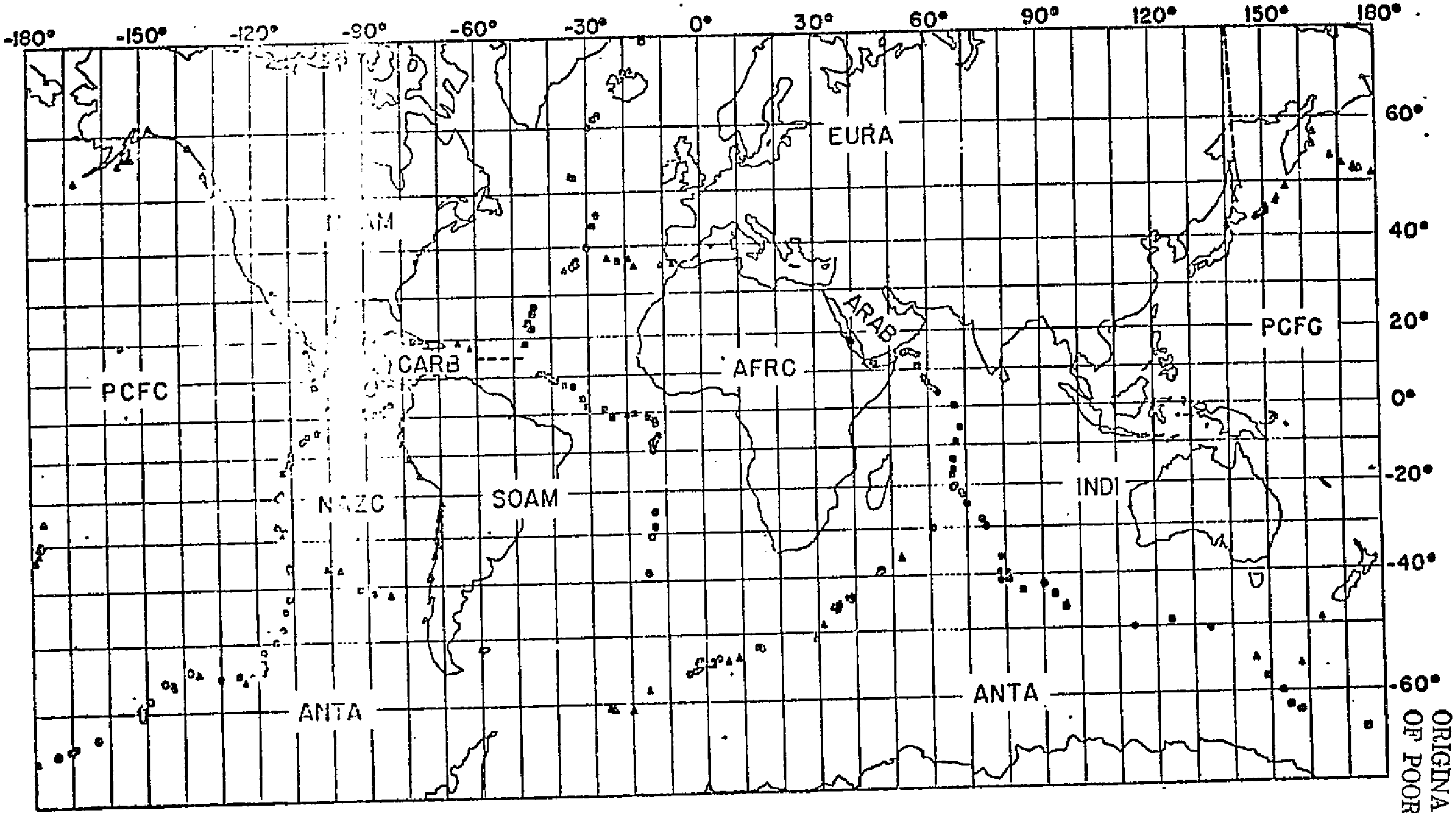

Figure 1.

ORIGINAL PAGE IS
OF POOR QUALITY

ORIGINAL PAGE IS
OF POOR QUALITY

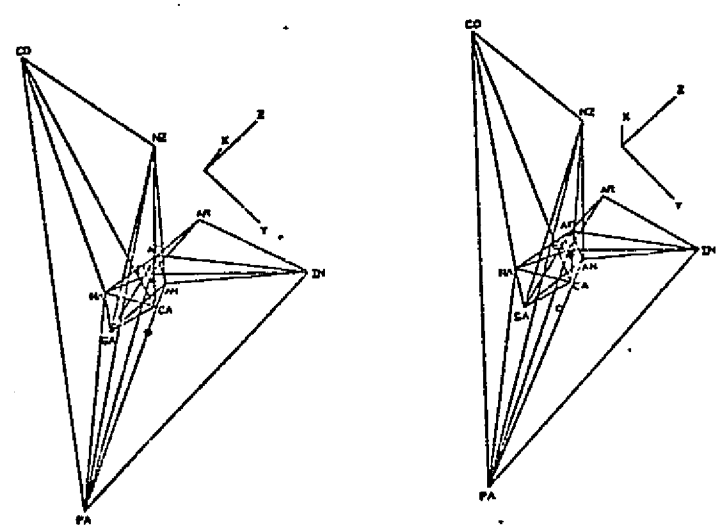

Fig. 2

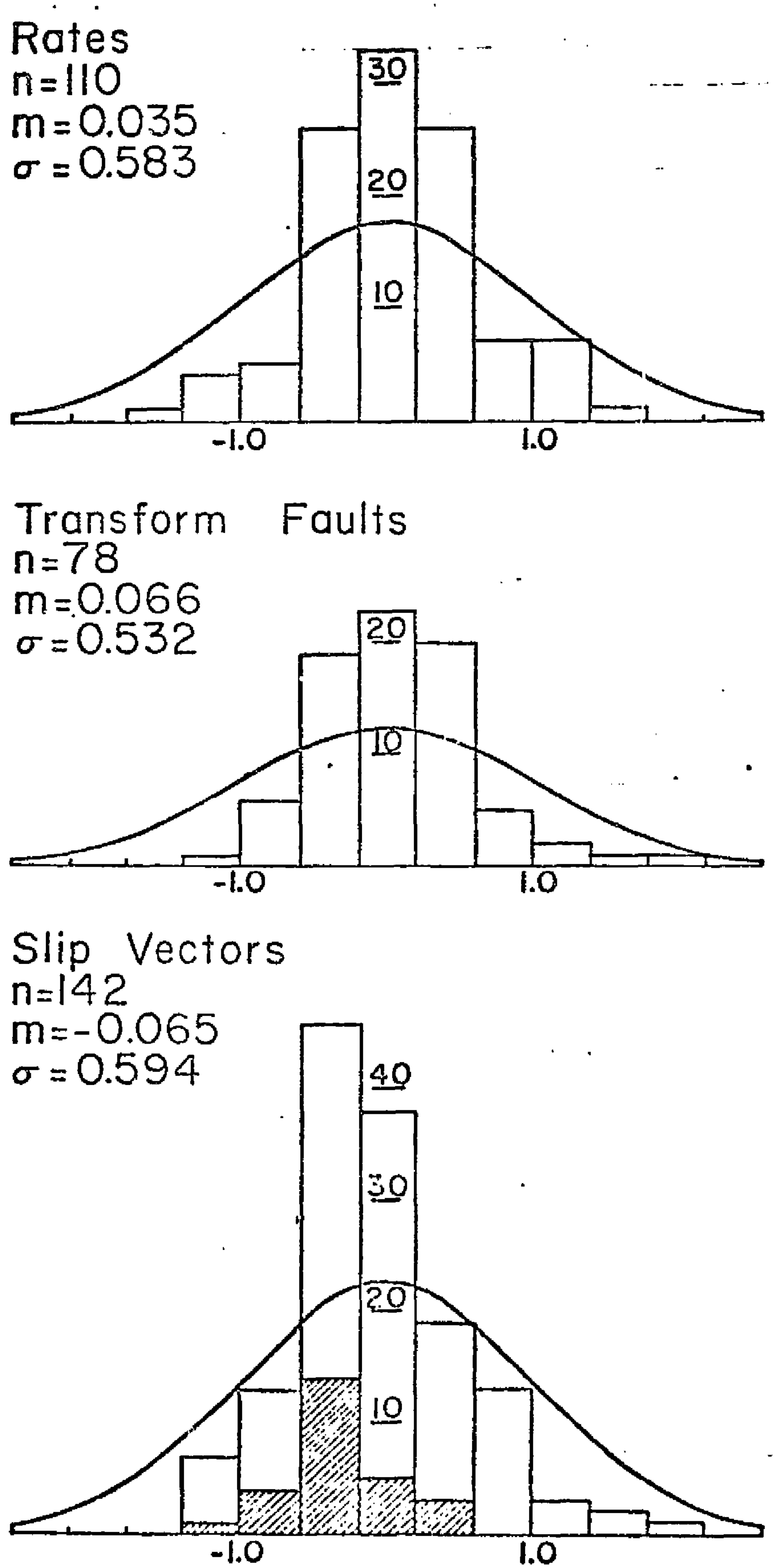

Rates
n=110
m=0.035
σ=0.583
30
20
10
-1.0
1.0
Transform Faults
n=78
m=0.066
σ=0.532
20
10
-1.0
1.0
Slip Vectors
n=142
m=-0.065
σ=0.594
40
30
20
10
-1.0
1.0

Figure 3.

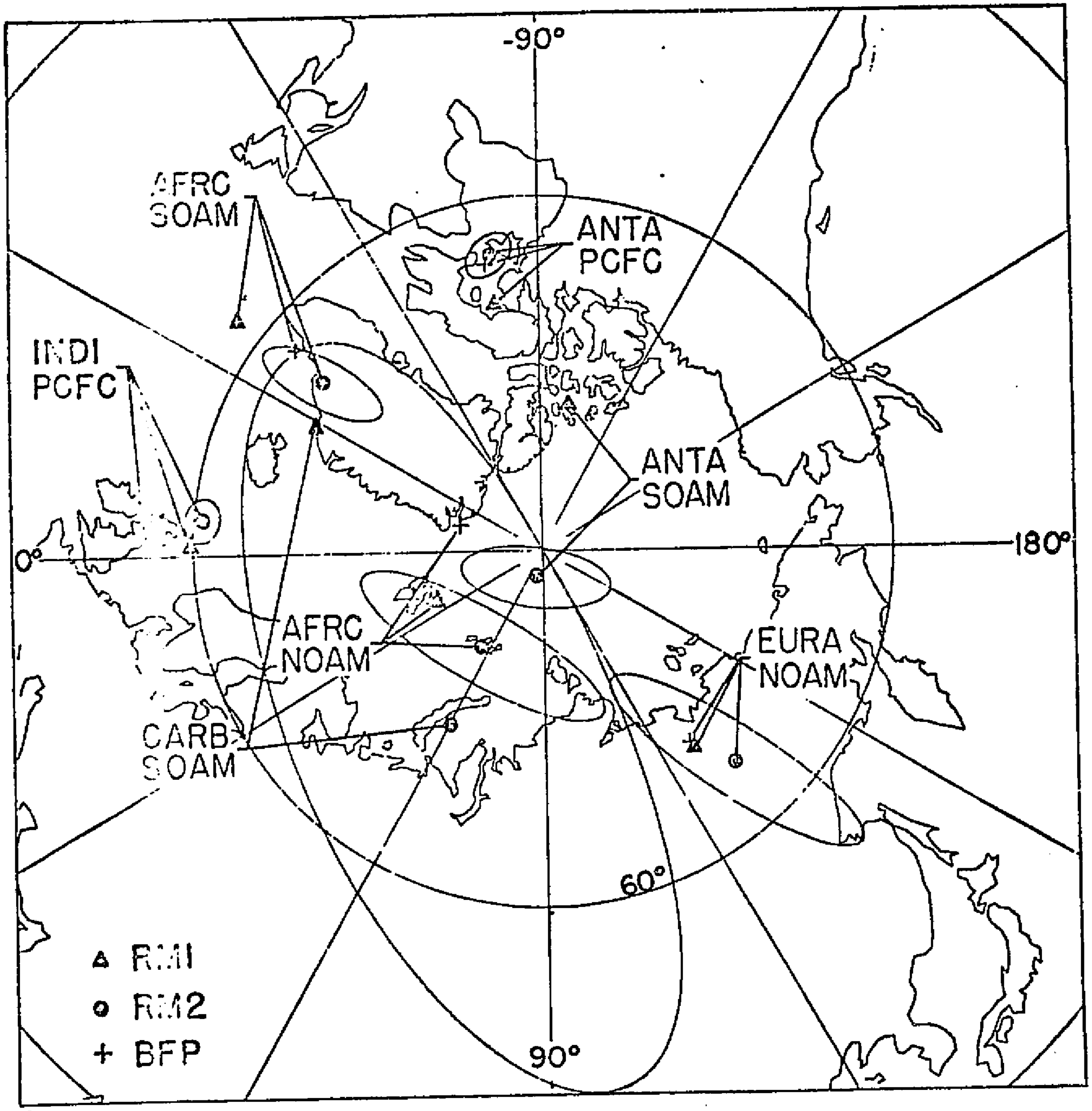
-90°
AFRC
SOAM
ANTA
PCFC
INDI
PCFC
ANTA
SOAM
0°
180°
AFRC
NOAM
EURA
NOAM
CARB
SOAM
60°
90°
RM1
RM2
BFP

Figure 4.

ORIGINAL PAGE IS
OF POOR QUALITY

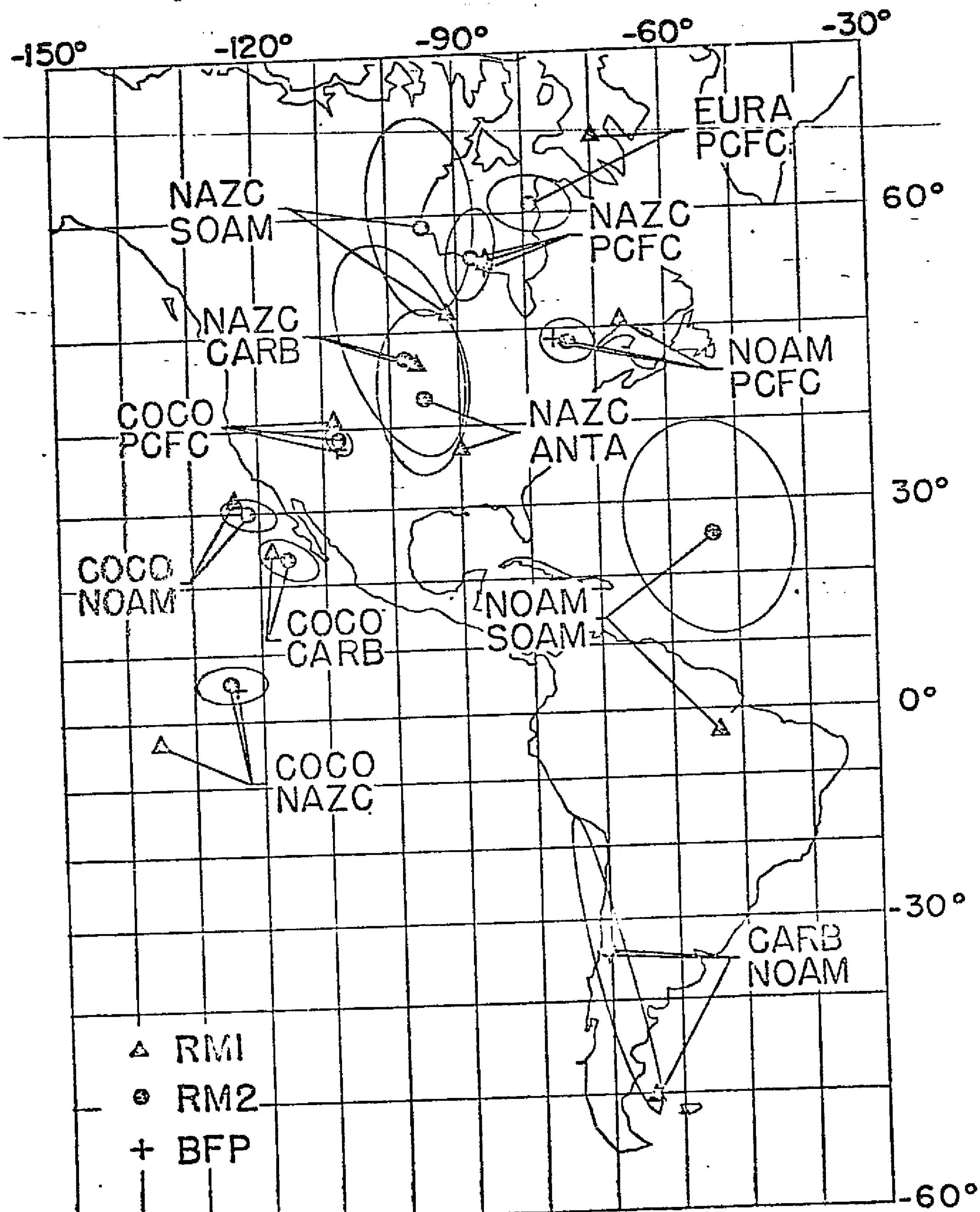

Figure 5.

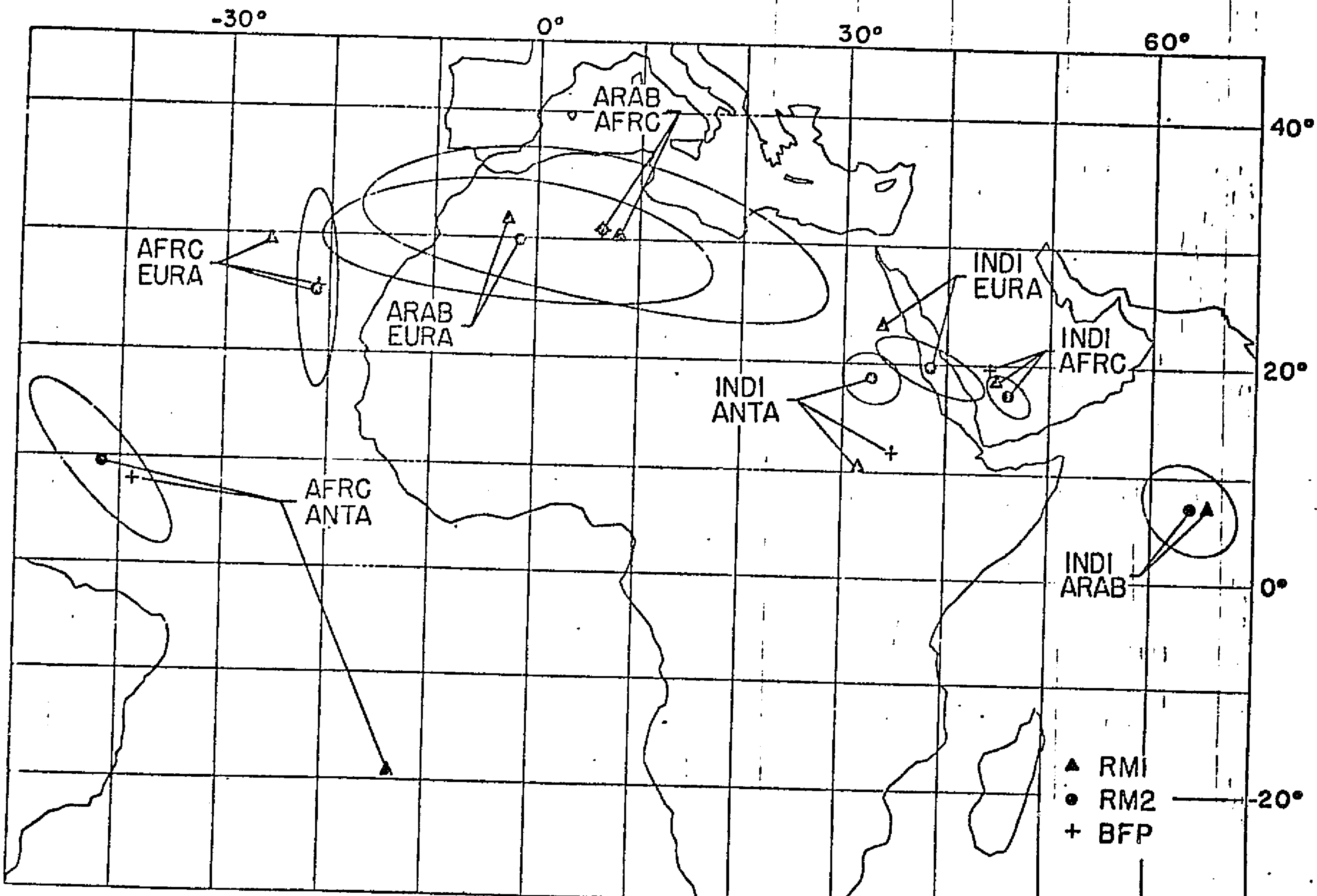

-30°
0°
30°
60°
40°
20°
0°
-20°
ARAB
AFRC
AFRC
EURA
ARAB
EURA
INDI
EURA
INDI
AFRC
INDI
ANTA
AFRC
ANTA
INDI
ARAB
RMI
RM2
BFP

Figure 6.

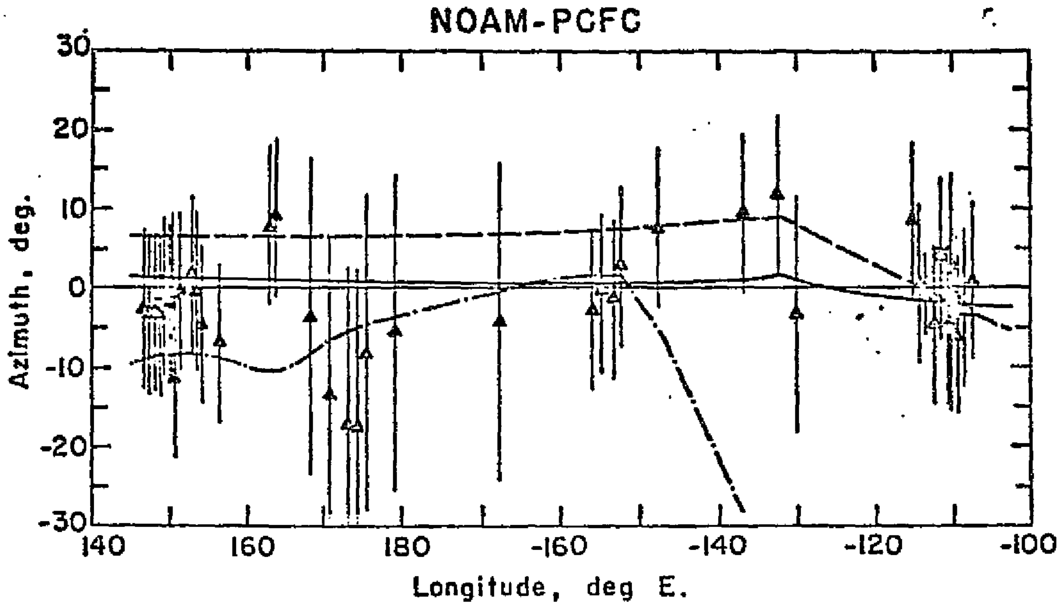

Figure 7.

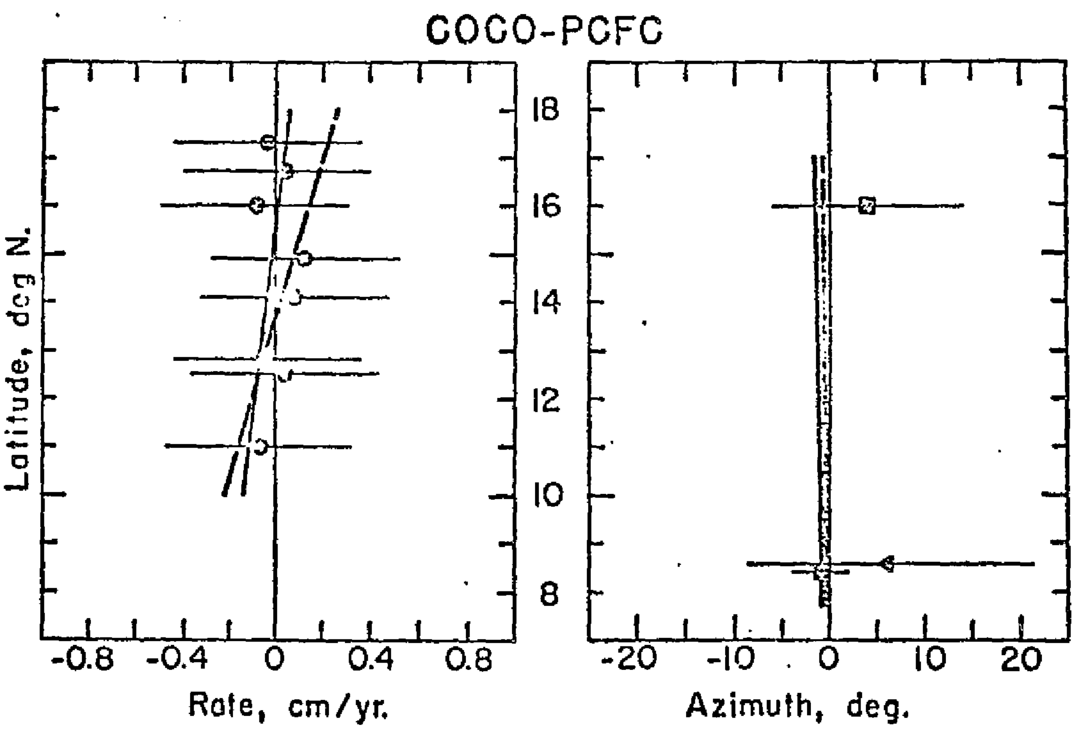

Figure 8.

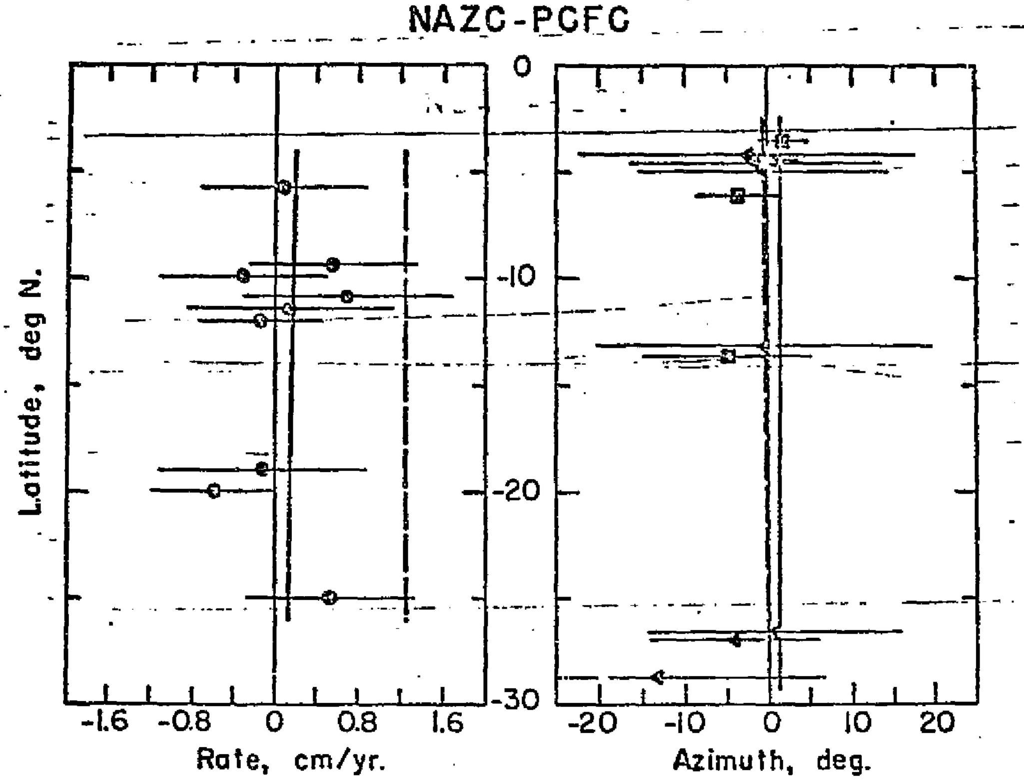

Figure 9.

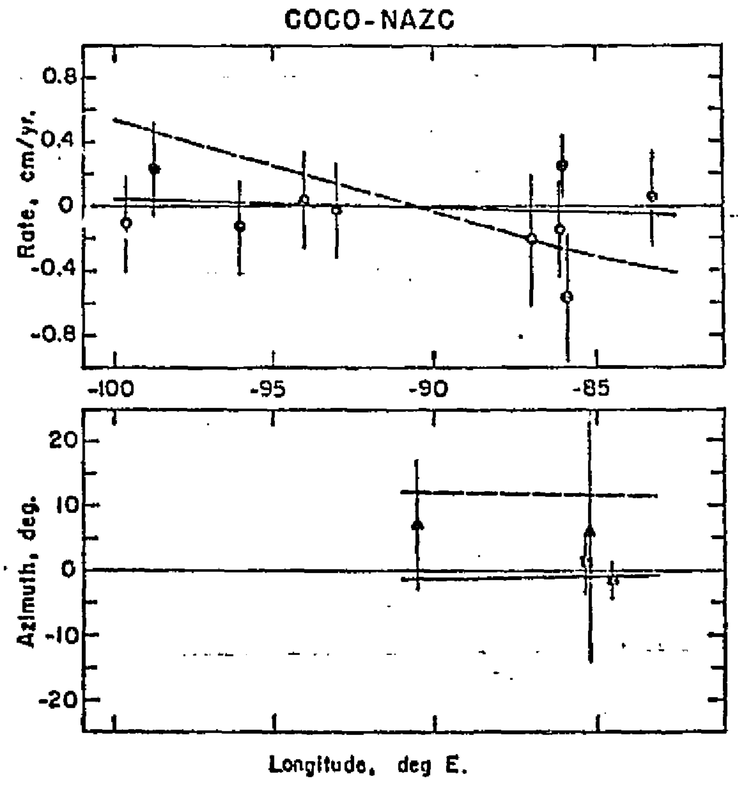

Figure 10.

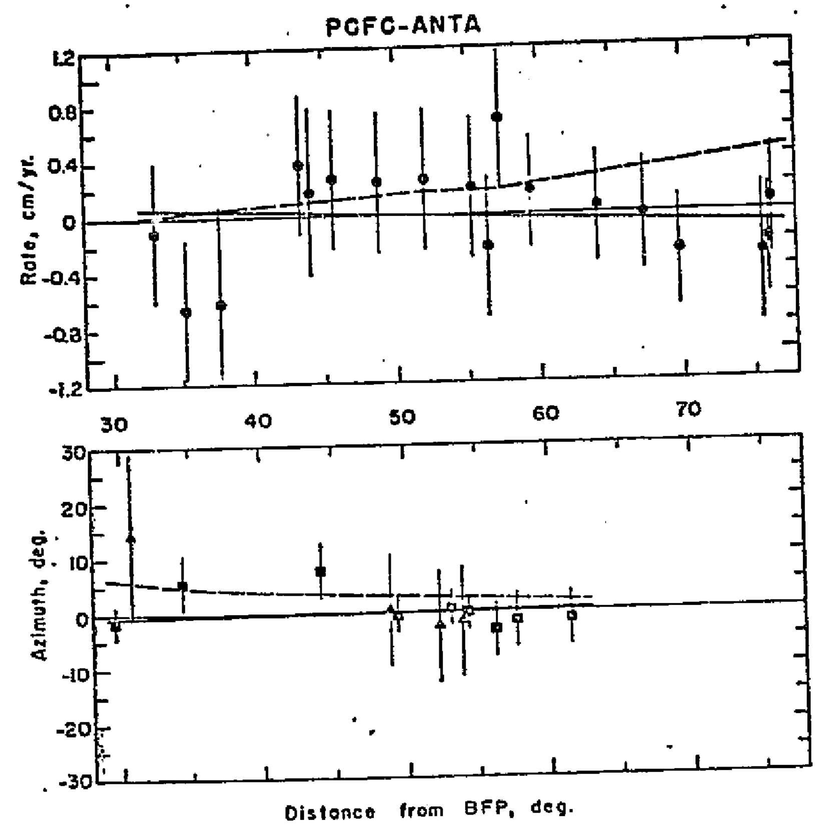

Figure 11.

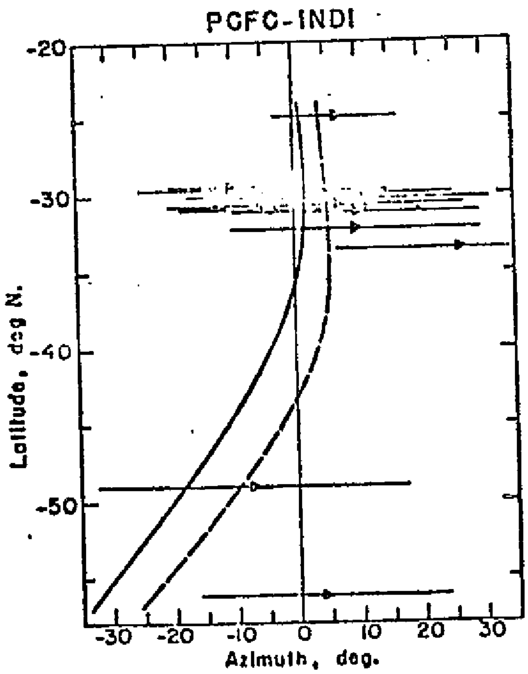

Figure 12.

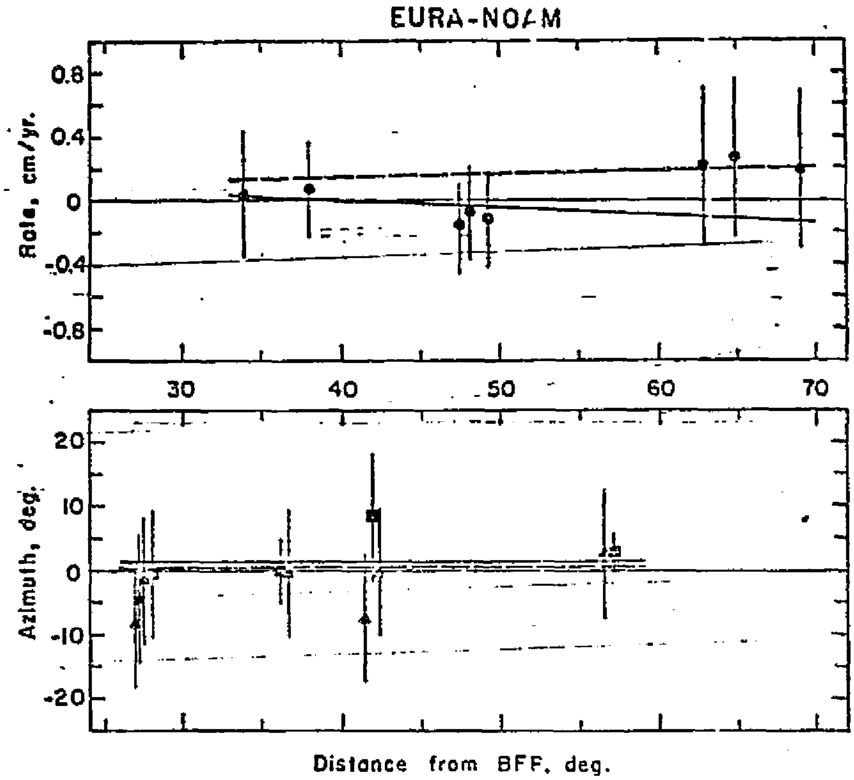

Figure 13.

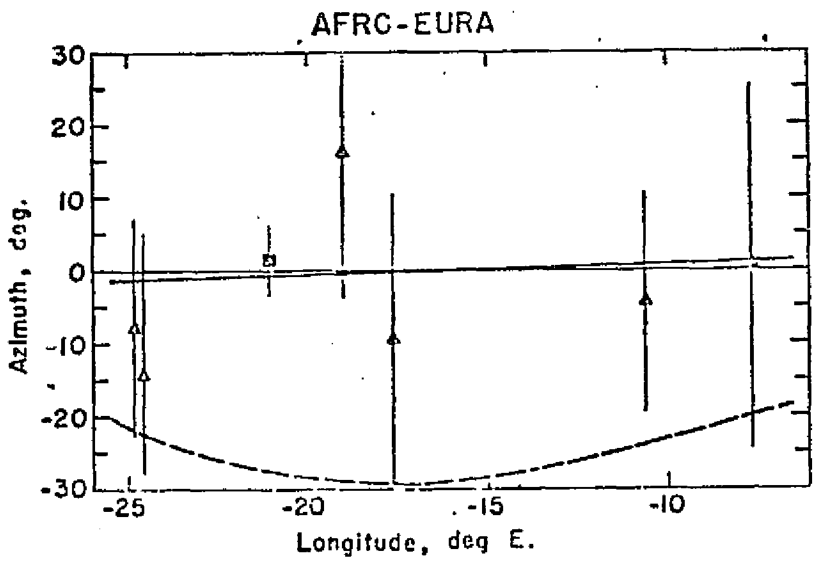

Figure 14.

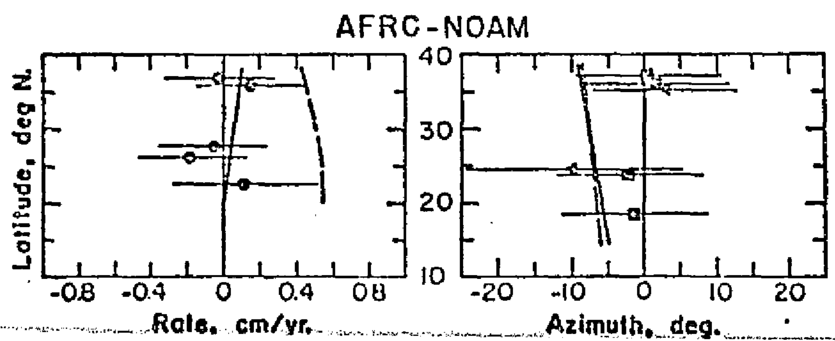

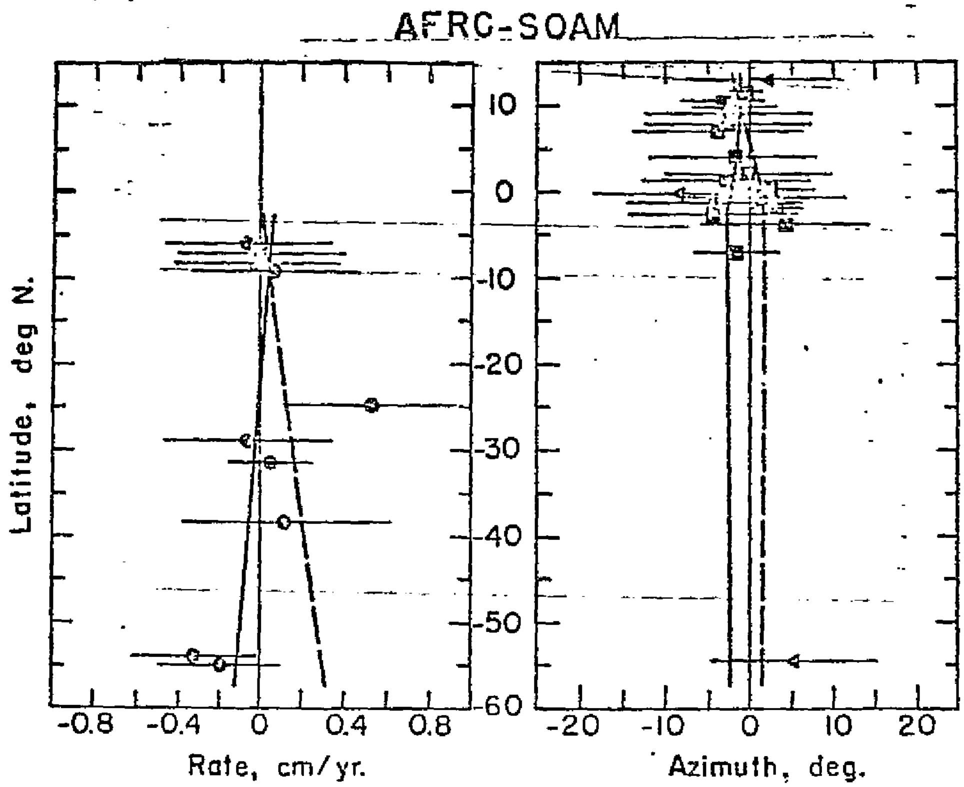

Figure 16.

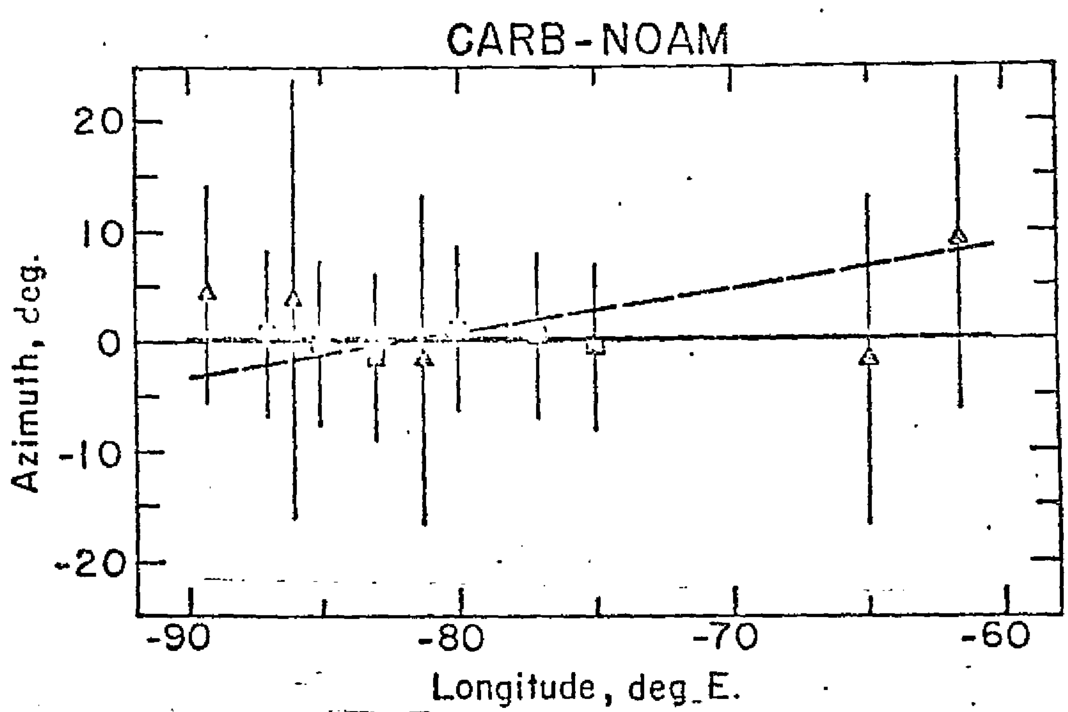

Figure 17.

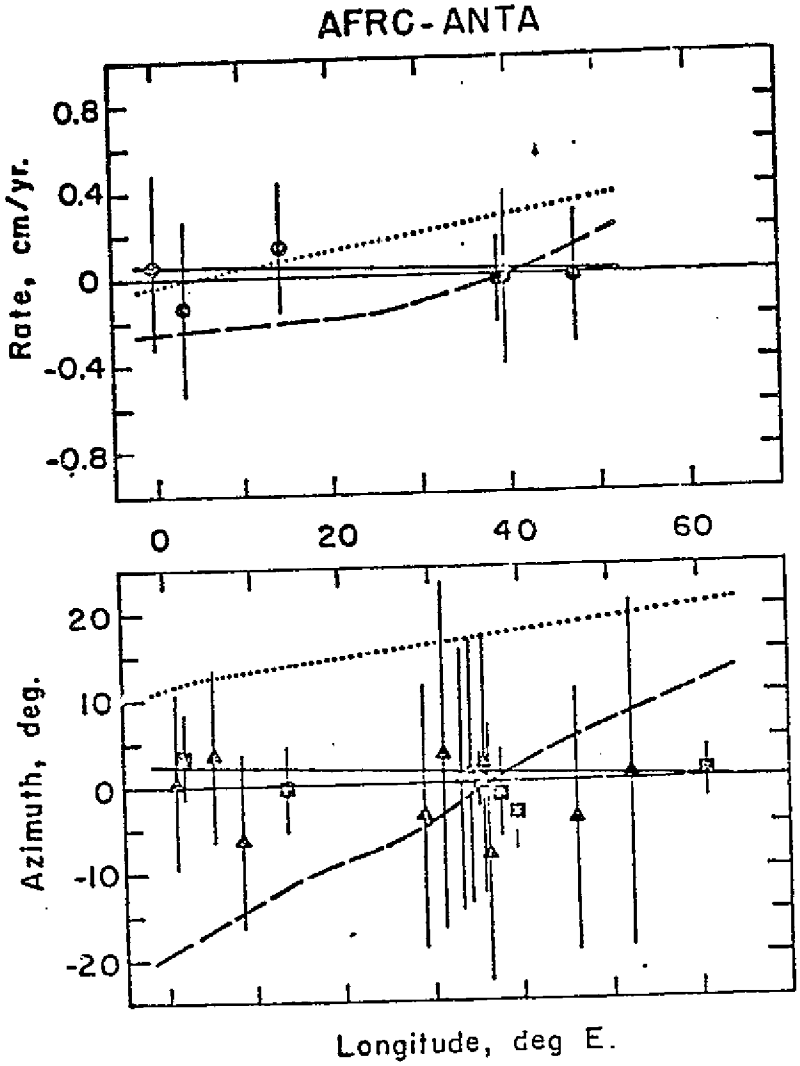

Figure 18.

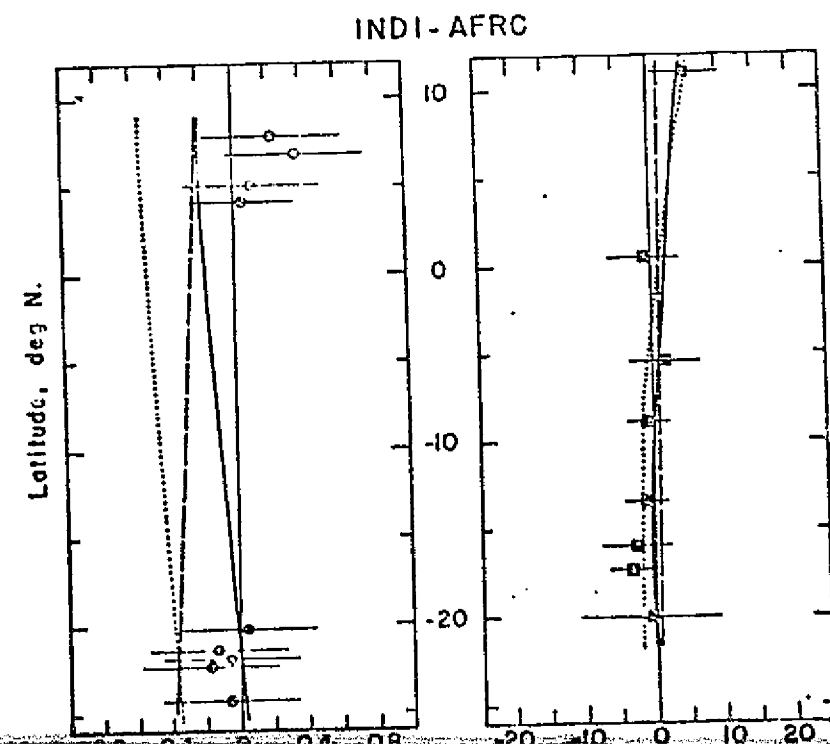

Figure 19.

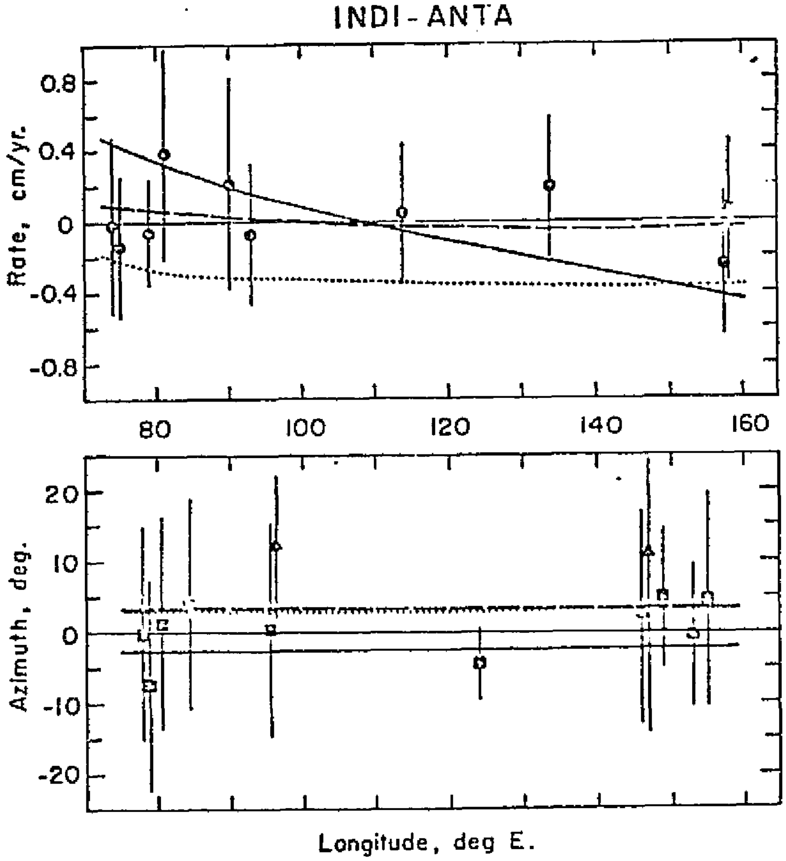
INDI-ANTA
Rate, cm/yr.
0.8
0.4
0
-0.4
-0.8
80
100
120
140
160
Azimuth, deg.
20
10
0
-10
-20
Longitude, deg E.

Figure 20.